Mediterranean Tropical-Like Cyclones forecasts and analysis using the ECMWF Ensemble Forecasting System (IFS) with physical parameterizations perturbations

Miriam Saraceni[1], Lorenzo Silvestri[2], Peter Bechtold[3], and Paolina Bongioannini Cerlini[4]

[1,2]Department of Civil and Environmental Engineering, University of Perugia, Perugia, Italy
[4]Department of Physics and Geology, University of Perugia, Perugia, Italy
[3]European Centre for Medium-Range Weather Forecasts, Bonn, Germany

Correspondence: Miriam Saraceni (miriam.saraceni@unipg.it)

Abstract. Mediterranean Tropical-Like Cyclones, called "medicanes", present a multiscale nature and their track and intensity have been recognized as highly sensitive to large-scale atmospheric forcing and diabatic heating as represented by the physical parameterizations in numerical weather prediction. Here, we analyse the structure and investigate the predictability of medicanes with the aid of the European Centre for Medium-Range Weather Forecast (ECMWF) Integrated Forecast System (IFS) ensemble forecasting system with 25 perturbed members at 9 km horizontal resolution (compared to the 16 km operational resolution). The IFS ensemble system includes the representation of initial uncertainties from the ensemble data assimilation (EDA) and a recently developed uncertainty representation of the model physics with perturbed parameters (Stochastically Perturbed Parameterizations, SPP). The focus is on three medicanes, Ianos, Zorbas and Trixie, among the strongest in recent years. In particular, we have carried out separate ensemble simulations with initial perturbations, full physics SPP, with a reduced set of SPP, where only convection is perturbed to highlight the convective nature of medicanes and an operational ensemble combining the SPP and the initial perturbations. It is found that compared to the operational analysis and satellite rainfall data, the forecasts reproduce the tropical-like features of these cyclones. Furthermore, the SPP simulations compare to the initial condition perturbation ensemble, in terms of tracking, intensity, precipitation and more generally in terms of ensemble skill and spread. Moreover, the study confirms that similar processes are at play in the development of the investigated three medicanes, in that the predictability of these cyclones is linked not only to the prediction of the precursor events (namely the deep cut-off low) but also to the interaction of the upper-level advected Potential Vorticity (PV) streamer with the tropospheric PV anomaly that is diabatically produced by latent heat.

1 Introduction

The Mediterranean region is a small but geographically complex area characterized by sharp land and sea transitions and surrounded by high mountain ranges. It is known for its frequent cyclogenesis. A small number of the intense cyclones that originate in the region present tropical-like features (Flaounas et al., 2022). They are a very significant phenomenon, due to their visual similarity with tropical cyclones, and while they are typically shorter-lived than North Atlantic hurricanes, they

may exhibit several tropical-like characteristics in their mature phase, such as a high degree of axial symmetry, a warm core, a tendency to weaken after making landfall, and a cloud-free "eye" at the center of the storm of mostly calm weather, as inferred from satellite images. Such vortices are better known as Tropical-Like Cyclones or Mediterranean hurricanes (medicanes). Medicanes have been documented in the Mediterranean region since the beginning of the satellite era (Ernst and Matson, 1983) and have been associated with polar lows (Rasmussen and Zick, 1987). These storms pose a significant threat due to their intense winds, heavy rainfall, and associated flooding.

Medicanes features have been commonly reported in the literature (Cavicchia et al., 2014; Romero and Emanuel, 2013; Emanuel, 2005; Zhang et al., 2019; Miglietta and Rotunno, 2019). They occur very infrequently, with an average of about 1/2 events per year over the entire Mediterranean region. They are most commonly formed in the western Mediterranean and the area between the Ionian Sea and the North African coast. Medicanes have a distinct seasonal pattern, with a peak at the start of winter, a significant number of events during fall, a few during spring, and very little activity in summer. As pointed out by Miglietta and Rotunno (2019) they only have a lifespan of a few days due to the limited size of the Mediterranean Sea, which is their main source of energy. Furthermore, they only exhibit fully tropical characteristics for a short period, with extratropical features predominating for most of their lifetime (Miglietta and Rotunno, 2019).

Medicanes differ from other Mediterranean cyclones in the complexity of their formation and evolution. However, unlike hurricanes, which develop in regions with near-zero baroclinicity and draw their energy from warm tropical oceans, medicanes form from pressure lows under moderate to strong baroclinicity, which is a typical condition of midlatitudes and Mediterranean cyclogenesis. Indeed, medicanes are regarded as baroclinic cyclones evolving into vortices with structural characteristics similar to tropical cyclones (Flaounas et al., 2022). The debate is still open on which processes sustain the cyclone development, baroclinic instability or pure diabatic forcing which also marks the tropical transition phase (Flaounas et al., 2022; Miglietta and Rotunno, 2019; Flaounas et al., 2021).

Typically, the initial phase of a medicane life cycle is similar to that of an extratropical cyclone, where the medicane intensifies through the interaction of an upper tropospheric disturbance (Potential Vorticity streamer (Flaounas et al., 2015)) with a low-level baroclinic area. However, their development is what makes them different given the relative contribution of large-scale forcing, air-sea interactions, and convection at different stages of their lifetime. Recently a classification has been produced for this type of phenomenon by Miglietta and Rotunno (2019) and Dafis et al. (2020). Medicanes have been grouped into three categories: those where baroclinic instability plays an essential role throughout the cyclones' lifetime and most of their intensification can be attributed to convection; those where baroclinicity is relevant only in the initial stage, and, the theory of wind-induced surface heat exchange (WISHE (Emanuel, 1986)) can explain their intensification through positive feedback between latent heat release and air–sea interactions, although WISHE may only take place after the occurrence of tropical transition, i.e. after organized convection near the cyclone centre is capable of sustaining the vortex; and finally those,

including smaller-scale vortices, that develop within the circulation associated with a synoptic-scale cyclone.

For this study three medicanes, among the strongest in recent years, were chosen: Ianos (September 15-20, 2020), Zorbas (September 27-31, 2018), and Trixie (October 28-November 1, 2016). The three medicanes have been selected because they are very different from each other, with Trixie being the weakest but also the longest lasting of the three (Di Muzio et al., 2019; Dafis et al., 2020) and generally among the longest lasting medicanes, Zorbas one of the shortest-lived and presenting high variability in predictability, as documented by Portmann et al. (2020) and Ianos one of the most intense medicanes ever observed, reaching category 2 hurricane status (Lagouvardos et al., 2022). As reported in the literature the three cyclones' origin is linked to the presence of upper-level cutoff low (Comellas Prat et al., 2021) associated with a potential vorticity streamer (Portmann et al., 2020). There, is suggested that the formation of the cyclone was accompanied by an anomalous value of SST of nearly 1.5 °C (at least in the cases of Ianos (Comellas Prat et al., 2021) and Zorbas (Portmann et al., 2020)). Moreover, the three cyclones acquired tropical-like characteristics in their lifetime: Ianos between the 17th and the 18th of September 2020 (Panegrossi et al., 2023), Zorbas on the 28th of September 2018 (Dafis et al., 2020) and Trixie during the 30th (Dafis et al., 2020). Nonetheless, besides these similarities, the convective activity and processes of intensification that pertain to each cyclone have been recognized to be different in the literature. Dafis et al. (2020) pointed out that Zorbas and Trixie showed long-lasting and organized convective activity close to the centre preceding the maximum cyclone intensity, while Ianos showed deep convection and precipitating clouds close to the center during the maximum cyclone intensity (Lagouvardos et al., 2022). Furthermore, there might have been a different contribution in the intensification of the cyclones by baroclinic and diabatic processes, with Ianos influenced mostly by diabatic processes in its intense phase (Comellas Prat et al., 2021) and Zorbas and Trixie developing in a baroclinic environment where convection possibly having a secondary role (Dafis et al., 2020).

Because of their small size, low frequency of occurrence (Cavicchia et al., 2014), and the complex geography of the Mediterranean region, predicting medicanes is a challenge for numerical weather forecasting. There are some climatological studies on medicanes, using synthetic production of tracks and 3D numerical simulation (Romero and Emanuel, 2013; Cavicchia et al., 2014; Zhang et al., 2019) which have assessed the climatological medicanes number per year, seasonal pattern, areas of occurrence and intensity. There are fewer studies based on observations (Pytharoulis et al., 2000; Moscatello et al., 2008; Miglietta et al., 2013) given the above-mentioned low frequency of occurrence and scarcity of data, which were focused on the analysis of medicanes convective activity. Numerous modeling studies of medicanes using convective permitting models and general circulation models include Davolio et al. (2009); Miglietta et al. (2011, 2013); Mazza et al. (2017); Cioni et al. (2016); Ricchi et al. (2019) with the importance of model resolution discussed in the review paper by Flaounas et al. (2022). Among the others, Carrió et al. (2020) was able to capture, with high-resolution modeling (2.5 km) the development of a small-scale cyclone and its relationship to convection, especially highlighting the role of diabatic heating in its intensification. Cioni et al. (2018) found out that explicit convection is necessary to capture the track, intensity, and thermal structure of a specific medicane in 2014. However, in the above-mentioned review paper, it is concluded that: "...a systematic gain from kilometer-scale resolution has not been generally demonstrated for cyclones yet".

Lastly, there have been relatively few studies that have analyzed medicanes using ensemble forecasts (Chaboureau et al., 2012; Mazza et al., 2017) and more specifically, by using the ECMWF ensemble forecasting system (Pantillon et al., 2013; Di Muzio et al., 2019; Portmann et al., 2020). Nonetheless, the ensemble forecast of ECMWF has proven to be a useful tool for predicting extreme weather events (Buizza and Hollingsworth, 2002; Buizza, 2008; Magnusson et al., 2015), for analyzing tropical cyclones (Torn and Cook, 2013) and their predictability (Munsell et al., 2013). Moreover, the model has demonstrated high predictive skill also for medicanes (Di Muzio et al., 2019). Pantillon et al. (2013) used ECMWF operational ensemble forecasts to study the predictability of a medicane in 2006 and found that they were more successful at consistently capturing early signals of its occurrence compared to ECMWF deterministic forecasts. However, Di Muzio et al. (2019), who used ECMWF ensemble forecasts to systematically analyze the predictability of medicanes, found that the ensemble members noted a marked drop in predictive skill beyond 5-7 lead days, indicating the existence of predictability barriers. Portmann et al. (2020) used ensemble forecasting to assess upstream uncertainties in the prediction of medicanes, also finding that the uncertainties were reduced with initialization closer to the medicane occurrence.

Research conducted on medicanes with ensemble forecasting has generally been carried out through the use of the perturbations to initial conditions only, as in Di Muzio et al. (2019), without the use of parameterization perturbations, by means of any stochastically perturbed parameterization scheme. However, an important part of the uncertainty associated with forecasting comes from uncertainty related to the physics of the model. For these reasons, this present study is concerned with ensemble forecasting that takes into account not only the uncertainty of initial conditions but also the uncertainty of model parameters. We present an assessment of the prediction of medicanes, with the use, not only of the IFS operational ensemble forecasting system at ECMWF, with initial conditions perturbation, but using also the physical parameterization perturbations, the Stochastically Perturbed Parameterizations (SPP) ensemble forecast. Indeed, this is a novel stochastic representation of model uncertainties which is still under development at ECMWF in order to replace the Stochastically Perturbed Parameterization Tendency scheme (SPPT) (Palmer et al., 2009). SPP consists of a set of physical parameters in the model being perturbed (Ollinaho et al., 2017). The added value of SPP is that it perturbs the amplitude and the shape of the tendencies from the individual physical processes, thereby also allowing for the generation of clouds and convection, thus it does not only perturb the amplitude of the total physics tendency as with SPPT. Leutbecher et al. (2017) and Lang et al. (2021) report on skillful forecast with SPP in the ECMWF ensemble system including for tropical cyclones, where SPP increases the spread of the tropical cyclone core pressure while presenting similar statistics to SPPT for the cyclone tracks. As discussed in Frogner et al. (2022) ensemble applications using SPP are clearly on the rise as it allows the representation of uncertainty close to the actual source of error and maintains physical consistency, particularly with local conservation of energy and humidity (Lang et al., 2021).

Thus, a comparison between three ensemble forecast experiments is set up. One ensemble is run with only initial condition perturbations, through the Ensemble Data Assimilation (EDA), one is run with the entire physical parameterizations perturbed and one is run with only the convective parameterization perturbed. The last experiment comprises both the initial conditions

and the model parameterizations perturbations. Each of these experiments is applied to the three above-mentioned chosen medicanes and the goal of this study is to determine whether these forecasts can accurately predict them, if there are possible biases presented by the ensemble forecasts and if the ensembles compare in terms of spread and error. Furthermore, the assessment of which of the perturbation experiments can capture the medicane more accurately is carried out trying also to understand what diabatic processes, among the ones already studied in the literature, influence the forecast and how different ensembles predict these.

The outline of the paper is the following. In Section 2 the data and methods used are described, with an in-depth description of the ensemble forecast experiments carried out, a description of the SPP, of the tracking method, and of the Hart (2003) diagnostic. In Section 3 the assessment of the ensemble predictions of medicanes in terms of tracking, intensity, precipitation, and thermal structure is presented. Then, in Section 5 the relevant process involved in the evolution and prediction of the medicanes are investigated in relation to the results of the previous sections and in Section 6, the results are discussed and the concluding remarks are given.

2 Data and Methods

2.1 Ensemble Forecast Simulation

For this work, the ensemble forecast experiments with the ECMWF IFS (Cycle 47r3: ECMWF,(IFS Documentation CY47R3, 2021b)) and the ECMWF operational analysis have been used. Both the ensemble forecast and the operational analysis have a $\simeq 9$ km horizontal grid spacing (TCo1279, for a more in-depth description of the horizontal grid, see Malardel et al. (2016)) and 137 levels in the vertical. The duration of the simulations used in this work is 9 days. Three different sets of experiments have been conducted, all of them consisting of a 24-member ensemble. The ensemble forecasts are initialized, amounting to 3 initial dates, each day at 0000 UTC. For Ianos the three dates are the 15th, the 16th, and the 17th of September 2020, for Zorbas the three dates are the 25th, the 26th, and the 27th of September 2018 and for Trixie, the three dates are the 25th, the 26th, and the 27th of October 2016. The three dates were chosen as three days before the intensification phase of each cyclone, based on the reference data of ERA5 reanalysis. Regarding the physical parameterization, a detailed description can be found in the IFS documentation (IFS Documentation CY47R3, 2021a).

The ensemble forecast is coupled to the ECMWF Wave Model (ecWAM:(IFS Documentation CY47R3, 2021c)) and to the Nucleus for European Modelling of the Ocean (NEMO) ocean model (Mogensen et al., 2012). The ecWAM model provides the atmospheric model with the Charnock parameter, thus controlling the sea surface fluxes via the surface roughness. The atmospheric oceanic surface heat and moisture fluxes are controlled by the SSTs computed from NEMO every 20 minutes using a 0.25° horizontal grid with 75 vertical levels. Due to the limited horizontal resolution of NEMO, the IFS is forced in the middle latitudes only, with fixed SSTs from the OSTIA product (Donlon et al., 2012) up to day 4, while beyond day 4 the SSTs from NEMO are used. The different types of experiments that have been carried out are reported in Table 1.

Table 1. Description of the different ensemble forecast experiments

Experiment ID	Experiment Setup
INI	Initial perturbations only - no model uncertainty representation
$SPP-Conv$	No initial perturbations - convective parameterization uncertainty representation
SPP	No initial perturbations - physical parameterizations uncertainty representation
TOT	Initial perturbations - physical parameterizations uncertainty representation

The first experiment is the ensemble forecast with initial condition perturbation only (INI experiment). This is done by adding perturbation to a 4D-Var (Rabier et al., 2000) analysis. The perturbations are constructed from an ensemble of 4D-Var data assimilations (Ensemble Data Assimilation, EDA, (Buizza et al., 2008)) where the size of the initial perturbations stems from the analysis uncertainty due to observation errors and model uncertainties including SPPT in the trajectory of the variational data assimilation. The second and third sets of experiments are conducted by running the ensemble with SPP applied. In the former (SPP-Conv) only the convective parameterization parameters are perturbed. In the latter (SPP), the convective, radiative, clouds and large-scale precipitation, turbulence, diffusion, and sub-grid orography parameterization parameters of the IFS model are perturbed, as briefly discussed below. In the last experiment (TOT) the operational forecast conditions of ECMWF are tested by including both the initial condition perturbation and the physical parameterizations perturbation.

2.2 Stochastically Perturbed Parameterizations Ensemble

The Stochastically Perturbed Parameterizations scheme represents model uncertainty in numerical weather prediction by introducing stochastic perturbations into the physical parameterization schemes (Lang et al., 2021) as mentioned above. SPP is a new scheme, aimed at replacing the currently used Stochastically Perturbed Parameterization Tendency scheme (SPPT) (Palmer et al., 2009) in the ECMWF ensemble forecast in June 2023. The new scheme, developed by Ollinaho et al. (2017), following the work of Baker et al. (2014) and Christensen et al. (2015), is based on applying perturbations directly to a selected number of parameters and/or equations within the parameterization schemes, usually those known to be specific sources of uncertainty for the model. The perturbations follow horizontal patterns that evolve stochastically in space and time. Each perturbed parameter is assigned an individual random field and different random fields are statistically independent. The log-normal distribution has been chosen for practical reasons as it ensures that the perturbed parameter values retain their original sign. The implementation of SPP allows the simultaneous perturbation of up to 27 parameters and variables in the deterministic IFS parametrizations of turbulent diffusion (Köhler et al., 2011), sub-grid orography (Beljaars et al., 2004), convection (Tiedtke, 1989; Bechtold et al., 2008), cloud processes and large-scale precipitation (Tiedtke, 1993; Forbes et al., 2011), and radiation (ecRad, (Hogan and Bozzo, 2018)). These 27 parameters and variables are reported in Supplementary Tables 1 to

4, together with a detailed explanation of the choices behind their perturbation. As mentioned above, the SPP perturbation is applied through a 2D random field generator. In its implementation, SPP uses a single scale with a decorrelation length scale of 1,000 km and a decorrelation time of 3 days (Fig. 1 of Lang et al. (2021)).

2.3 Validation Data

In order to analyze the predictive skill of the ensemble, besides the operational analysis, the ensemble forecast perturbation experiments have been compared with the satellite-based, globally-gridded Global Precipitation Measurement (GPM) Integrated Multi-satellite Retrievals for GPM (IMERG) (Huffman et al., 2020). In GPM-IMERG, the retrievals from geostationary satellites are blended seamlessly with information from the passive microwave (PMW) sensors from low-orbit satellites. this is done in order to achieve both a high accuracy and a high temporal (30 min) and spatial ($\simeq$ 10 km) resolution since the precipitation estimation based on the PMW alone suffers from a low sampling rate. Furthermore, the data are also calibrated by using rain gauges at the ground level. In this research, the 24-hour accumulated precipitation values are used. The latter data are provided at the same resolution, $0.1°$, as in the ensemble simulation.

2.4 Cyclone tracking

The method described here has been used to evaluate the tracks for both operational analyses, used as verification and ensemble forecasts. The tracking method is based on Picornell et al. (2014) and Ragone et al. (2018). The algorithm first aims at finding the local minima of the sea level pressure field at each time step. Then, for each minimum, the sea level pressure gradient of the sea level pressure along eight main directions (E, NE, N, NW, W, SW, S, SE) within a circle of radius 200 km is computed. The computed gradient is then chosen to be lower than $5hPa/200km$ in at least 6 directions. After the minimum detection and filtering via selection through sea level pressure gradient, a proximity condition is applied to construct the complete trajectory. Starting from the first time step, each minimum is connected to the following one, at the following time step, that satisfies the condition of being closer than $\Delta x = V\Delta t$, with $V = 50km/h$ and $\Delta t = 3h$. If this condition is met, the two consecutive minima are considered to belong to the same trajectory. This condition was considered suitable and chosen according to the results of Ragone et al. (2018). Once the trajectories have been found, only the trajectories that last longer than 24 hours and those that spend more than 12 hours over the sea are selected. Trajectories that spend less than half their time over land or within 100 kilometers of the coast are discarded.

2.5 Hart Parameters

To analyze these three storms, the thermal structure, and the thermal asymmetry have been investigated. The chosen parameter to quantify the latter has been recognized in the upper-level thermal wind, $-V_T^U$, which is considered to be a relevant parameter in distinguishing tropical-like cyclones from fully baroclinic cyclones (Mazza et al., 2017), and secondly on the thermal asymmetry, B. These parameters belong to the three-dimensional cyclone phase space diagnostic introduced by Hart (2003).

There, the thermal asymmetry is defined as the storm-motion-relative 900–600 hPa thickness asymmetry across the cyclone within its radius:

$$B = (\overline{Z_{600\,hPa} - Z_{900\,hPa}}|_R - \overline{Z_{600\,hPa} - Z_{900\,hPa}}|_L) \tag{1}$$

where Z is the geopotential height, R indicates the right of current storm motion, L indicates the left of storm motion, and the overbar indicates the areal mean over a semicircle around the cyclone centre.

Instead, the cyclone's upper-level thermal structure (i.e., its cold or warm core) is indicated by $-V_T^U$. If it attains a positive sign, the cyclone attains an upper-level warm core. Indeed the $-V_T^U$ is defined as:

$$-|V_T^U| = \frac{\partial(\Delta Z)}{\partial ln(p)}\Big|_{600\,hPa}^{300\,hPa} \tag{2}$$

The two pressure levels have been changed from 600 hPa to 700 hPa and from 300 hPa to 400 hPa due to the lower height of the tropopause in the midlatitudes with respect to the tropics (Picornell et al., 2014). These values are computed within a 200 km radius around the detected cyclone center by using the geopotential height field. In the Hart (2003) formulation, this radius was chosen to be 500 km, but given the smaller size of medicanes compared to tropical cyclones (Miglietta et al., 2013), the radius used in this study is smaller, 200 km. Since a positive value of lower-level thermal wind, $-V_T^L$, can characterize not only medicanes but also extratropical cyclones with warm seclusion (Hart, 2003), we consider important only the upper-level thermal wind, $-V_T^U$. In the case of the thermal asymmetry, the threshold value of $B = 10\,m$ has been determined by analyzing ECMWF reanalyses ERA40 at $1.125°$ of the resolution, from which no major hurricane (winds of greater than 210 km/h) had associated with it a value of B that exceeded 10 m (Hart and Evans, 2001). Even if the threshold value of *B* has been originally determined for larger tropical/extratropical cyclones, previous studies have shown that such value is also useful in the case of medicanes (Miglietta et al., 2011). The deep warm core phase is represented by the asymmetry *B* being lower than 10 and closer to 0 and by a highly positive value of $-V_T^U$.

3 Overview of the Storms

A summary of the main features as retrieved by the analysis data: the storm duration, the period, the region of occurrence, the asymmetry *B*, and upper-level thermal wind $-V_T^U$ is provided in Table 2. The latter two parameters have been used for the computation of the cyclone phase space diagrams. The intensity (central pressure) and trajectory of each storm are shown in Fig. 1 along with the ensemble track.

The three storms formed and developed in the same area, the Southern Mediterranean, in the Ionian and Aegean Seas. This region has one of the highest medicanes occurrences, as recognized in the literature (Cavicchia et al., 2014; Zhang et al., 2021). They occurred in the same period of the year, between September and November, the most frequent period for medicane occurrence (Romero and Emanuel, 2013). From Fig. 1 it can be gathered that there are some differences in duration and intensity, with Trixie being the longest-lasting of the three medicanes (in terms of the deepening phase) and Zorbas and Ianos being

Table 2. Duration, region of occurrence, central pressure, CP, asymmetry parameter, B, and upper-level thermal wind from the operational analysis for each storm. The upper-level thermal wind, $-V_T^U$ and the thermal asymmetry parameter, B represent the parameters from the cyclone phase-space of (Hart, 2003).

Storm	Region	Period	Duration (d)	CP (hPa)	B	$-V_T^U$
Ianos	SM	September 2020	7	994	0	73
Zorbas	SM	September/October 2018	5	993	4	39
Trixie	SM	October 2016	4	1009	2	38

*SM = Southern Mediterranean

deeper than Trixie, as mentioned in the Introduction. As the track suggests (Fig. 1a) Ianos originated in the Gulf of Sidra. Then between the 14th and 15th of September 2020, it emerged in the Gulf of Sidra and spent most of its life over the Mediterranean Sea, eventually reaching Greece on the 17th and turning southeastward, dissipating around the 21st. The analysis is capable of reproducing a value similar to the observed pressure minimum of 995 hPa (Comellas Prat et al., 2021).

Zorbas formed on the 27th of September 2018 close to North Africa and then moved into the central Mediterranean, turning eastward and moving over Greece into the Aegean Sea, where it finally decayed four days after its formation (Fig. 1d). Zorbas reached its maximum intensity (observed 992 hPa), which is well captured by the analysis.

Medicane Trixie formed on the 28th of October 2016. On the 29th, it moved to the east of Malta, then on the 30th of October, it moved eastward towards Greece (Fig. 1g) while dissipating. In the analysis, there was only a short intensification period evident, and the minimum pressure was fluctuating between 1010 and 1014 hPa during the period from the 29th and the 30th of October, which might have been highly underestimated.

4 Results: Ensemble forecast evaluation

This section examines the ensemble forecast experiments for certain aspects that are crucial for cyclones. The focus is put on the cyclones track, the cyclones intensity, as measured by central pressure (this value is considered the most stable and robust metric for assessing the intensity of a cyclone on a global scale (Davis, 2018)), the cyclones precipitation and thermal structure. The chosen parameters to quantify the latter are the above-mentioned upper-level thermal wind, $-V_T^U$ and thermal asymmetry, B. Finally, the tropical-like phase of these cyclones is thoroughly investigated.

4.1 Tracking

The ensemble tracking results are reported in Fig. 1. As examples, the tracks starting from the 16th of September are shown for Ianos, the ones starting from the 27th of September are shown for Zorbas, and the ones starting from the 27th of October are shown for Trixie.
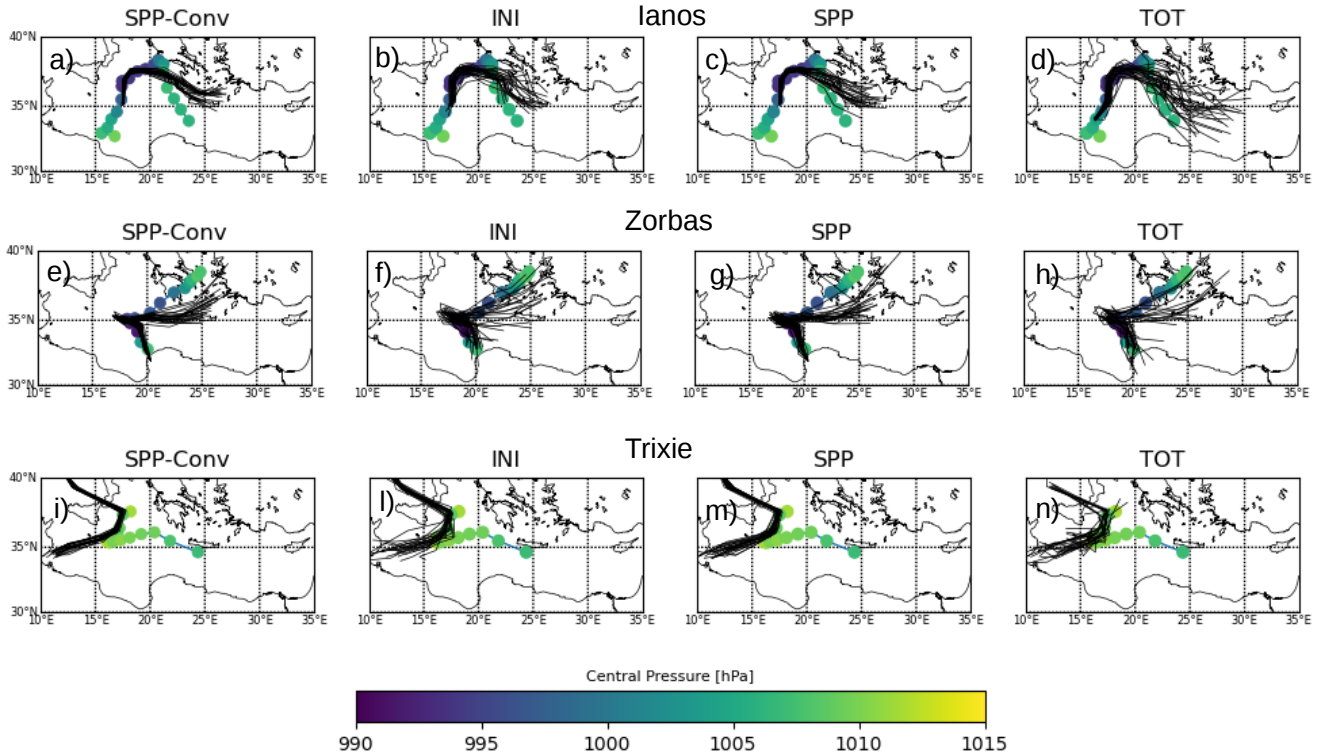
Figure 1. Track of the three storms for the operational analysis as reference track and for the ensemble members belonging to each experiment (SPP-Conv on the first column, INI on the second column, SPP on the third column and TOT in the fourth column) for the three storms, Ianos in a, b, c and d, Zorbas in e, f, g and h and Trixie in i, l, m and n. As background the operational analysis is reported with the colour representing the intensity, meaning the central pressure in hPa. For Ianos the experiments starting on the 16/09 have been chosen, for Zorbas the ones starting on the 27/09 and for Trixie the ones starting from the 27/10.

By looking at Fig. 1a to d and Fig. 1e to h the ensemble tracks follow the references for Ianos and for Zorbas. On the contrary for Trixie, the tracking, which starts one day prior to the starting date of the reference track (starting on the 28th) follows the track until the 29th early hours (Fig. 1i to n) when it diverges and ends up in North Africa, underlying a missed forecast. This is consistent also for earlier starting dates (the 25th and the 26th) with a greater error in terms of initial position (not shown). Fig. 1 shows that, as expected, the simulations with initial conditions perturbations (INI and TOT) tend to show more spread in the initial position. However, the spread at later stages in the simulation seems to be similar for both the INI experiment and the two experiments with the physics perturbation, SPP, and SPP-Conv, while on the other hand, the TOT experiment shows a slightly higher spread than the others simulations.

For Ianos the 16th of September was chosen as an example, but the behavior for the three starting dates is quite similar, with the trajectory being reproduced quite well for the first days and the error increasing with time. The latter is calculated as the

root mean square error between the ensemble mean track and the reference track. It never exceeds 300 km (not shown) and is always below 100 km up to 48 hours (not shown). The error values are similar in all three experiments, but slightly lower for the INI and TOT experiment. In the case of Zorbas and Trixie, since the starting dates are earlier than the start of the reference track, the earlier the simulations start, the greater the uncertainty in the start position, and hence the greater the spread. Fig. 1 shows the latest simulated starting dates for all cyclones. For Zorbas, starting on the 27th, the obtained tracks follow the reference with a small error, at least for the first days, which is anyway always below 300 km in later stages. As in the case of Ianos, the error made by the four experiments is similar. For Trixie, the error goes up to 700/800 km for the four experiments with respect to the 27th, the last start date shown in figure 1g, h, and i.

The tracking results shown in Fig. 1 are mirrored by the ensemble spread and the relationship between the spread and the error presented in Fig. 2 and Fig. 3 respectively. Following the approach of Hamill et al. (2011), the spread of the ensemble for a single cyclone ensemble forecast at a given forecast time is defined as:

$$S_l(t) = \frac{1}{n} \sum_{i=1}^{n} D_i \tag{3}$$

where D_i denotes the great-circle distance of the ith ensemble member position of the cyclone from the ensemble mean cyclone position. The total number of ensemble members used for the calculation is 24 and the spread has been computed for each starting date (3 dates for each medicane). The results, reported in Fig.2, are for the same start date as in Fig. 1, i.e. 16 September for Ianos, 27 September for Zorbas, and 27 October for Trixie, which is also representative of the spread of the other start dates. It is found that the TOT experiment has the largest mean track spread for the three cyclones (Fig.2 a), b) and c), but is comparable to the INI ensemble for most of the simulation period. The spread for the SPP and SPP-Conv ensembles is comparable and lower than the other two experiments but reaches a similar value to the INI ensemble at the end of the simulation. Ianos and Zorbas show less spread than Trixie at initialization, especially for the INI and TOT experiments (which are probably dominated by the initial perturbation at the beginning). This may be due to the fact that for Trixie, whose analysis track starts on 28 October (Fig.1g to 1i), there is a large uncertainty in the initial position. Looking at the spread-skill relationship (Fig. 3), measured by the ratio of the ensemble spread and the root mean square error between the ensemble mean track and the reference track, it can be said that as mentioned before the error is always larger of the ensemble spread and they are only comparable in the first hours of the simulations (20h to 40h) when the spread/skill values are closer to one. The SPP, the SPP-Conv and the INI are generally more under-dispersed than the TOT experiment in all three cases. The former three experiments behave generally in the same way, with the INI experiment showing less error after the second day for Ianos and Zorbas, but behaving similarly for Trixie. The TOT experiment performs better for Zorbas, but not for Trixie and Ianos.

At later forecast steps, Trixie is the cyclone with the highest spread for all three perturbations compared to Ianos and Zorbas. By looking at the general spread trends, while during the first two days of the simulations, the initial perturbations dominate the spread for all cases, by day 3 the spread from the physical parametrizations becomes equivalent. As a result the spread of the TOT ensemble, which is a combination of the two, tends to compare well with the INI ensemble at the beginning of the simulation and then to the SPP and SPP-Conv at later stages. The INI experiment spread is highest at initialization,
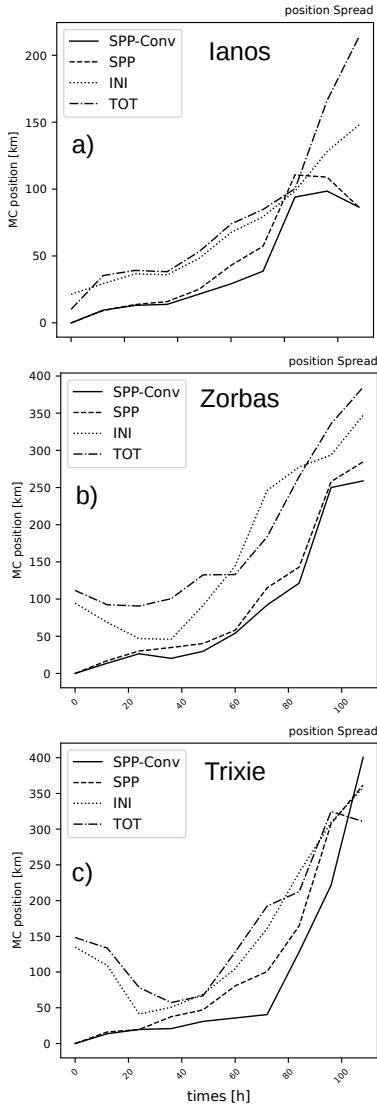
Figure 2. Mean ensemble spread of the medicanes track for each ensemble perturbation experiment for Ianos (a), Zorbas (b) and Trixie (c). The track spread is computed as described in Eq. 3 and is reported in km. For Ianos the experiments starting on the 16/09 have been chosen, for Zorbas the ones starting on the 27/09 and for Trixie the ones starting from the 27/10, in order to be consistent with the ensemble tracks shown in Fig. 1

as also seen in Lang et al. (2012), since the EDA perturbations are associated with a shift and intensification/weakening of the cyclone. Even considering the case-to-case variability, in terms of the spread of the track, the SPP-Conv experiment is the one with consistently less spread for all the cyclones. The low error values obtained by Ianos and Zorbas, compared to those obtained in the case of Trixie ($\geq$ 800 km), make it not only the medicane with the largest spread but also the one with

315 the most significant error. Indeed, it has been verified that this particular simulated cyclone deviates from the analysis track. The simulation track of Trixie is probably due to the fact that the ensemble forecast does not correctly capture the processes associated with cyclogenesis, but it can also be related to the fact that the simulations start too early before the appearance of the medicane. This is an aspect also recognized by (Di Muzio et al., 2019) in the simulation of these events.

Interestingly, both SPP experiments, and specifically the SPP-Conv, produce cyclone spread that is comparable at the later
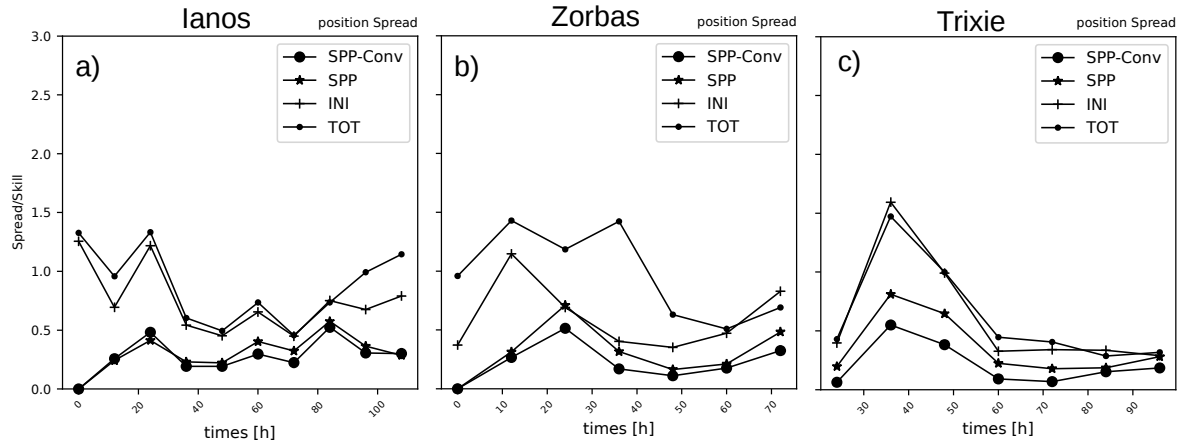
Figure 3. Ensemble Spread/skill relationship for each ensemble perturbation experiment for Ianos (a), Zorbas (b) and Trixie (c). The spread is computed as in Eq. 3 and the skill is the root mean squared error between the ensemble mean and the analysis tracks. For Ianos the experiments starting on the 16/09 have been chosen, for Zorbas the ones starting on the 27/09 and for Trixie the ones starting from the 27/10, in order to be consistent with the ensemble tracks shown in Figure 1.

320 stages of the simulation to the experiment with initial condition perturbations only. Similar results have been found in Lang et al. (2012), underlining the initial condition and physical heating-related sources of uncertainty in the tracking of these cyclones.

4.2 Intensity

The other important aspect investigated is the intensity of the cyclones analyzed. The intensity is assessed by studying the
325 minimum core pressure at the cyclone position.

The development of the core pressure with the simulations is reported in Fig. 4 where the mean sea level pressure at the centre of the cyclone (Minimum Core Pressure in Fig. 4) is shown, with the ensemble mean, the 25%-75% percentile and the 5%-95% percentile compared to the analysis for the three ensemble experiment for chosen starting dates, as an example. For Ianos there is an overestimation of the cyclone deepening (Fig. 4a, d, g and l), with a time shift of one day, compared to the
330 analysis, which is consistent in all three experiments. For Zorbas the minimum pressure is underestimated only in the case of the SPP-Conv experiment, however, there is a shift of 12 hours compared to the analysis in the three experiments (Fig. 4b, e, h and m). In the case of Trixie, there is an underestimation (Fig. 4c, f, i and n) and the ensemble experiments are not able to
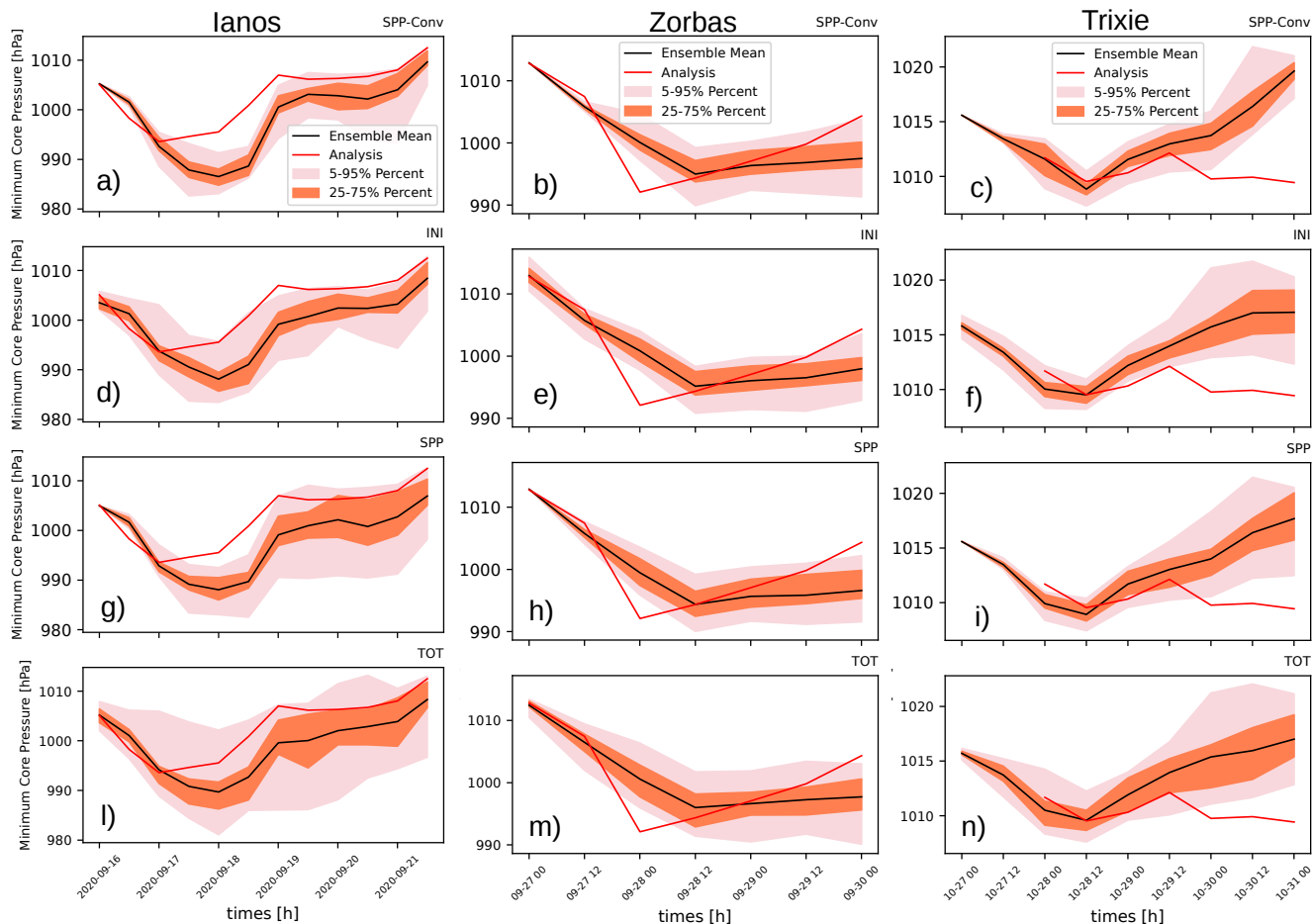
Figure 4. Analysis of the mean seal level central pressure, for Ianos in the first column, for Zorbas in the second column, and for Trixie in the third column. The plots show the ensemble members' development throughout the simulation. In each Fig. the ensemble mean is reported in black, the operational analysis is reported in red and the two shaded areas represent the 25-75 % percentile and the 9-95 % percentile. The SPP-Conv experiment is reported for each medicane in Fig. (a), (b), and (c). The INI experiment is reported in Fig. (d), (e) and (f), the SPP experiment in Fig. (g), (h) and (i) and the TOT experiment in (l), (m), (n).

capture the full evolution of the cyclone pressure (especially the second deepening around the 30th).

335   For all three cyclones, the spread is slightly higher for the SPP and the SPP-Conv experiments compared to the INI one, however, the TOT experiment is the one with the highest spread for the three cyclones. The reference analysis is included in the ensemble spread of the latter experiments (INI and TOT) compared to what happens with the SPP experiments, at least in the initial time steps. This is particularly true for Ianos (Fig. 4a, d, g and l). For Zorbas, the pressure deepening is slightly better captured by the SPP and the TOT ensembles (Fig. 4b, h and m). As pointed out before, there is a shift of the minimum

340 pressure of 12 to 24 hours compared to the analysis. For Ianos this is also present in the simulation starting on the 15th but is absent in the simulation starting on the 17th. This is due to the improved initial conditions when the forecast starts closer to the event. The same can be said for Zorbas. For Trixie, apart from the first deepening happening on the 28th of October, which is well captured by all the experiments, the second minimum, which is the deepest, is not captured by any of the experiments ensemble memebers, even when starting on the 27th of October (the last start date). In general, there is an underestimation of

345 the minimum core pressure, and its evolution up to the 29th is captured better by the TOT experiment, followed by the SPP experiment (Fig. 4i and n). Overall, the TOT ensemble, the operational forecast at ECMWF, perfors better in terms of core pressure, since it includes both the initial perturbation and the model perturbation.

4.3 Precipitation

The precipitation field has also been analyzed and verified against observation. The verification field is chosen to be the pre-

350 cipitation, as in Vich et al. (2011); Montani et al. (2011). Matching the forecast with the verifying data is hampered by the irregularly spaced ground network of observations and by the spatial variability of precipitation. Therefore, satellite products, in particular the above mentioned Integrated Multi-satellite Retrievals for GPM (GPM-IMERG), are used.

The precipitation structure of the three medicanes, in terms of intensity and position, is similar to what is observed in tropical

355 cyclones (Zhang et al., 2021, 2019). Indeed, there are similarities in their rainfall structures and those for Mediterranean cyclones (Flaounas et al., 2018) where most precipitation associated with medicanes is concentrated to the northeast side of the cyclone centre, as is shown in Figure 5 for the three cyclones. For the three cyclones, the ensemble mean of the last starting date is shown. For each cyclone, the daily accumulation on the day of the "tropical-like" phase is shown in Fig. 5. For Ianos this is the 17th of September, for Zorbas is the 28th of September, and for Trixie is the 28th of October. The daily accumulation

360 values from the ensemble forecast experiments are comparable to the observed values only regarding Ianos. In general, the maximum is better captured by the SPP experiments for Ianos (Fig. 5a and c), while for Zorbas and Trixie, this is true for the INI, the TOT and the SPP-Conv experiments (Fig. 5f, g, and i). The standard deviation of each ensemble experiment shows that there is higher uncertainty associated with the higher values of the precipitation distribution (Supplementary Fig. S1). This is consistent for all three cyclones. There is little difference between the SPP-Conv and the SPP experiment in terms of

365 precipitation distribution. This mirrors what was shown in Fig. 4.

The positioning of the maximum precipitation in the presented distributions (Fig. 5), is generally consistent with the observed GPM-IMERG distribution. However, there are some other secondary maximums in the distribution that are not well captured, for all three cyclones. This is possibly related to the simulation resolution not being able to capture completely the

370 precipitation structure. Preliminary results from the recent work of the Destination Earth (DestinE) project (Gascón et al., 2023) shows that the accumulated precipitation pattern is slightly better captured by the 4 km simulation compared to the 9 km one with the IFS model (https://confluence.ecmwf.int/x/w53m for Ianos, reported as an example).
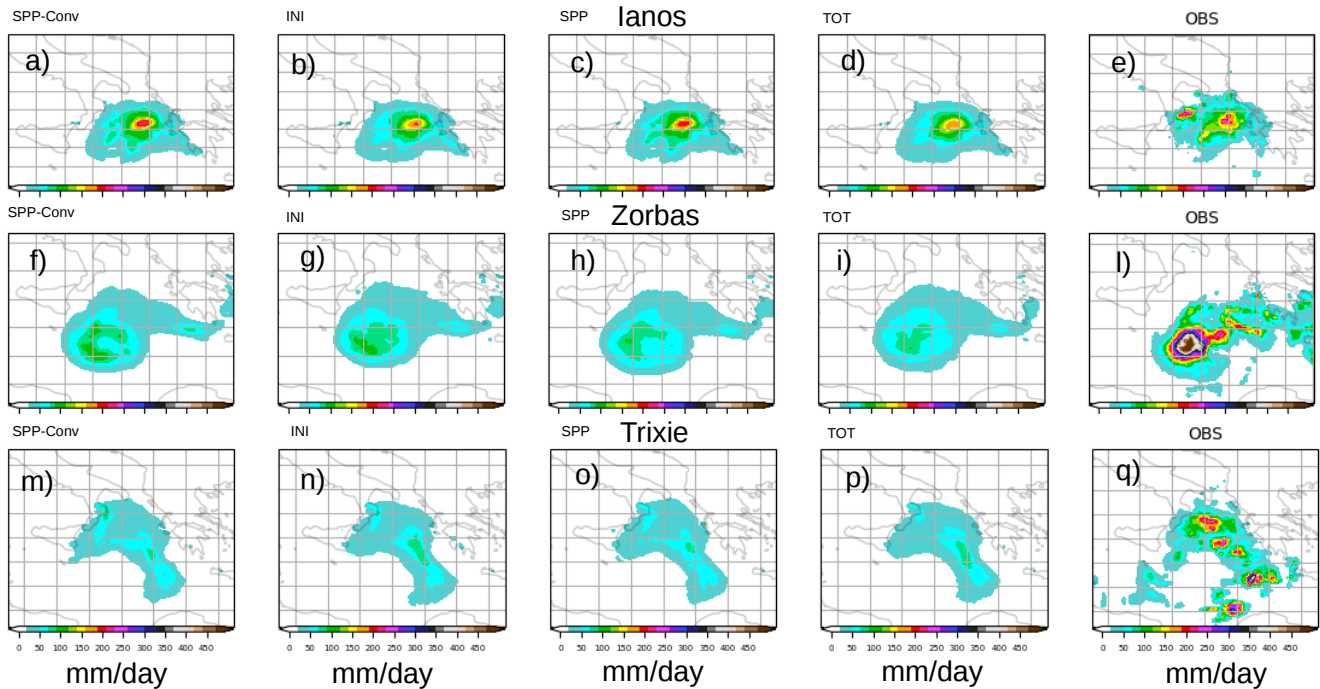
Figure 5. Daily accumulated precipitation (mm/day) for the three ensemble experiments ensemble means compared to the satellite observation GPM-IMERG. For Ianos the 17th is shown in Fig. (a), (b), (c), (d) and (e). For Zorbas the 28th is shown in Fig. (f), (g), (h), (i), and (l). For Trixie the 28th is shown in Fig. (m), (n) (o), (p) and (q). The SPP-Conv ensemble forecast accumulated precipitation is reported in the first column, the INI ensemble in the second column, the SPP ensemble in the third column, the TOT ensemble in the fourth column, and the observations in the fifth column. For Ianos the experiments starting on the 17th are shown, for Zorbas the ones starting on the 27th and for Trixie the ones starting from the 27th.

The daily accumulated precipitation shown in Fig. 5 belongs to the simulations with the latest starting date, where the
375 maximum precipitation is better captured. Indeed, the error in the simulated ensemble mean precipitation maximum compared to the observation is decreasing with the forecast start date closer to the medicane occurrence. This is specifically true for Ianos and Zorbas (as shown in Supplementary Fig. S2), while for Trixie, the maximum is also underestimated. For Trixie, the simulation is not able to capture the intensity of the precipitation. This is linked to the absence of the deepening of the cyclone and the precipitation starts to decrease sensibly after the 28th. This is seen within all the starting dates.
380 In the fourth column of Fig. 5, the TOT ensemble means are shown. The latter ensemble mean compares well to the INI ensemble, similar to what happens for the standard deviation of each ensemble experiment (Supplementary Fig. S1 and S2), thus confirming the results of the tracking and intensity.

4.4 Thermal structure and asymmetry

The Hart parameters, $-V_T^U$ and B, are analyzed in Fig. 6. We limit our physical analysis of the Hart parameters and the heating
385 and intensification to the experiments with either initial or physical perturbations. The focus is on the values where the cyclone deepening occurred in the observation, thus the values in Table 2 are reported as references in Fig. 6. The violin plots of the forecast distribution for each experiment at different starting dates are shown with the median (white dot) and the interquartile range (gray bar). The sections at the sides of each violin plot represent the kernel density estimation to show the shape of the distribution of the data (wider sections of the violin plot represent a higher probability that members of the population will take
390 on the given value; the thinner sections represent a lower probability). The choice for the violin plot was made because, unlike a box plot that can only show summary statistics, violin plots depict summary statistics and the density of each variable. In Fig. 6 only the SPP-Conv and the INI experiments are shown for comparison, because the results of the SPP experiments, as already pointed out above, are very similar to those obtained by the SPP-Conv.

395 The forecast distribution in the three ensemble experiments presents different behaviors compared with the analysis reference value (ref in Fig. 6) and with the starting date in the three experiments. In general, the three ensemble experiments can reproduce the thermal structure of the storms, showing in some cases a reduced spread with forecast start date closer to the occurrence, probably related to the fact that these starting dates coincide with the period in which the cyclone had already developed (see Fig. 6a and c for Ianos) and that the appearance of a symmetrical storm can benefit from improved initial con-
400 ditions (Di Muzio et al., 2019). This behavior is consistent for all three perturbation experiments.

The Ianos simulations show a reduced spread with later starting dates accompanied by the distribution value approaching the analysis value, for the thermal wind (Fig. 6a and c), and the thermal asymmetry (Fig. 6b and d). In particular, for the thermal asymmetry B, this makes the spread of the ensemble to be included below the threshold of 10 m which would define the system
405 as a frontal system rather than a non-frontal one (Miglietta et al., 2013), thus showing a better performance in reproducing the tropical-like phase of medicanes. This is true for both experiments, INI and SPP-Conv, as well as for Zorbas and Trixie. In the case of Zorbas, there is a usually smaller spread for the last starting date only regarding the thermal wind (Fig. 6e and g). Instead, there is a comparable spread for the thermal asymmetry, especially for the INI experiment (Fig. 6h). However, the forecast distribution of both experiments contains the reference analysis values for both the thermal wind and the thermal
410 asymmetry (Fig. 6e to h). In Trixie, the spread is comparable between the starting dates for the thermal asymmetry parameter and thermal wind (Fig.6i to n). There is a consistent underestimation of the thermal wind (with median values of $-V_T^U$ around -25 to -50), in all three ensemble experiments. The forecast distribution is closer to the analysis values ($-V_T^U = 39$) for the third starting date, for both ensemble experiments, as shown in Fig. 6i and m. This underestimation of the upper-level thermal wind means that a warm core was never reached in the ensemble forecast experiments, as it will be explored in the following sections.

415
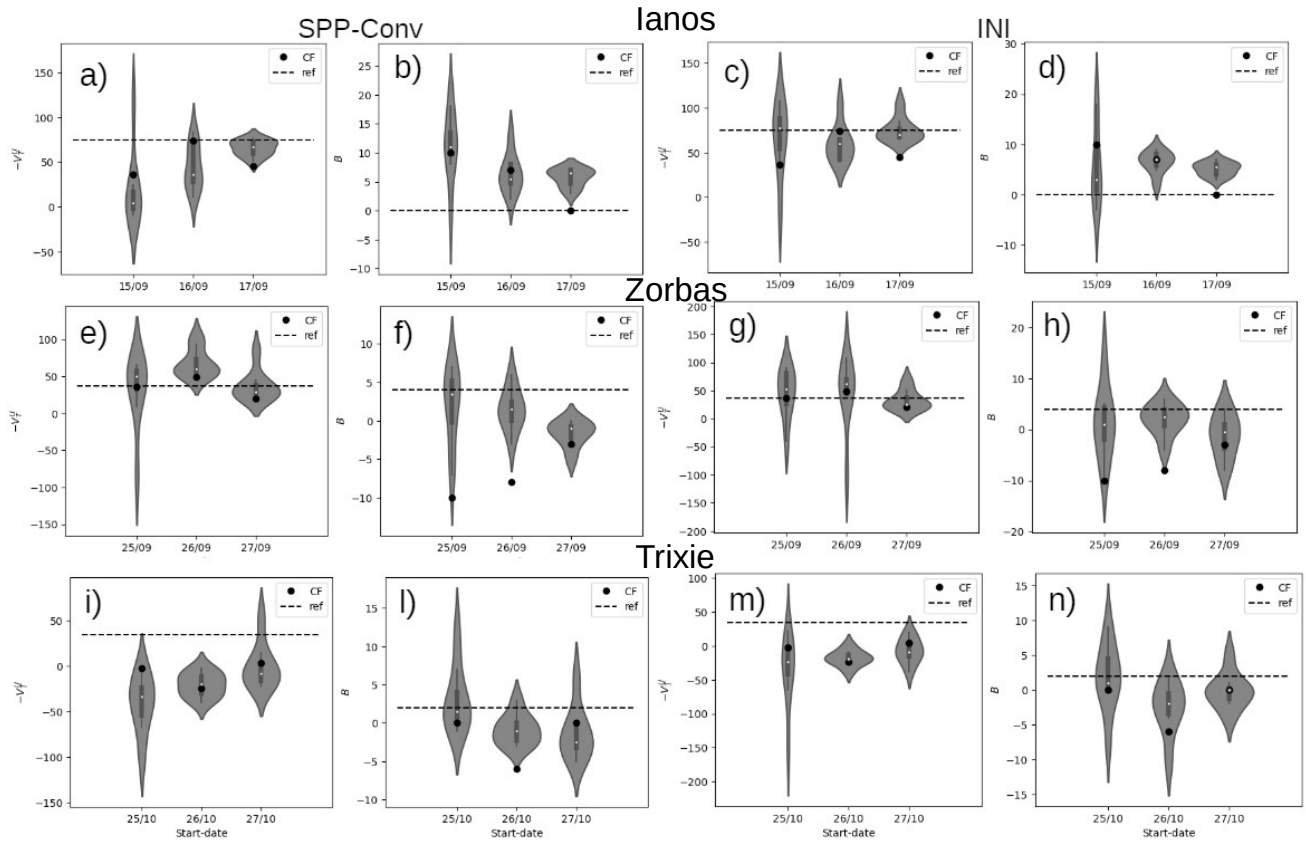
Figure 6. Ensemble forecasts violin plots of thermal wind, $-V_T^U$, and thermal symmetry, B, for each starting date for Ianos in Fig. (a) and (b) for the SPP-Conv ensemble forecast and in Fig. (c) and (d) for the INI ensemble forecast, for Zorbas in Fig. (e) and (f) for the SPP-Conv ensemble forecast and in Fig. (g) and (h) for the INI ensemble forecast and for Trixie in Fig. (i) and (l) for the SPP-Conv ensemble forecast and in Fig. (m) and (n) for the INI ensemble forecast. The violin plot is a hybrid of a box plot and a kernel density plot, which shows peaks in the data. The white dot represents the median, the thick gray bar in the center represents the interquartile range (25th-75th) and the thin gray line represents the rest of the distribution. On each side of the gray line is a kernel density estimation to show the distribution shape of the data.

5 Results: Physical processes analysis

To understand the processes of cyclone formation, intensification and tropical-like phase and how they affect the forecast, a comparison was made between the operational analysis and the ensembles. To reduce the amount of data, the analysis of the ensembles was reduced to consider a subset of 8 members, instead of 24.

5.1 Cyclones formation

The synoptic environment favoring cyclogenesis in the Mediterranean is the presence of a deep upper tropospheric trough, cut off from the large-scale circulation and intruding into the Mediterranean. The latter can bring thermodynamic disequilibrium, owing to its deep cold air (Emanuel, 2005; Flaounas et al., 2022). As the low approaches the Mediterranean environment with small baroclinicity, the air masses are lifted, decreasing the temperature above and increasing convective instability. The presence of an intrusion of very cold air in the upper troposphere may allow for the conversion from thermal energy into kinetic one (Palmen, 1948). This is usually accompanied by the presence of air masses with high potential vorticity (PV) intruding in the Mediterranean region (Flaounas et al., 2022), which usually triggers instability also in the case of extratropical cyclones (Flaounas et al., 2015; Raveh-Rubin and Flaounas, 2017). This stratospheric air mass can introduce anomalous high PV in the upper troposphere, which induces thermodynamic instability strengthening the surface vortex below. Usually, this stratospheric air mass intrusion is called PV streamer (Claud et al., 2010) and it is evidenced here that it is present in all three medicanes. This is underlined in Fig. 7a to c for the operational analysis in which the height of the isosurfaces of 2 PVU (PVU $= m^2 K kg^{-1} s^{-1} 10^{-6}$) is shown in relation to the mean sea level pressure for the three medicanes. These factors have already been found to be an integral part of Ianos and Zorbas formation in the literature, while for Trixie, to the authors knowledge, these aspects have never been fully analyzed. For Ianos, on 16 September the cut-off low was present (clearly identified at the 500-hPa level in Supplementary Fig. S3) and the PV streamer approached the area over the low center and wrapped around it (not shown), as also evidenced in Lagouvardos et al. (2022). Then, on 17 September, as it is shown in Fig. 7a the PV streamer broke up, resulting in the formation of a PV cutoff. Similarly, the formation of a PV streamer with the cutoff low already present (Supplementary Fig. S3) on 27 September over the Mediterranean was followed by cyclogenesis of Zorbas at the PV southeastern flank (Portmann et al., 2020), as it is shown in Fig. 7b, followed by a PV cutoff (not shown for the analysis but reported in Supplementary Fig. S6 for the ensemble experiments). For Trixie, the presence of a cutoff low on 28 October (Supplementary Fig. S3) is accompanied by the PV streamer reaching the area in which the cyclone is forming, even if the interaction between the PV streamer and the cyclone is not so evident (Fig. 7c). However, it is noted here that the PV cutoff is never reached (reported in Supplementary Fig. S6 for the ensemble experiments).

For Ianos in general, the PV streamer is well reproduced by the SPP-Conv and the other ensembles (not shown), especially regarding its interaction with the heating at 500 hPa (colored lines in Fig. 7d). However, on the 17th of September at 00 UTC the PV streamer detachment from the large-scale hasn't happened yet, as Fig. 7d shows, but it will happen 12 to 24 hours later (Supplementary Fig. S6) which is in line with what is shown in Fig. 4 regarding the simulated minimum central pressure reaching the lowest value with a delay compared to the analysis. This delay means that both in the analysis and the ensembles the medicane reaches its maximum intensity with the creation of the PV-cutoff, meaning that the former is dictated by the latter, at least for the timing. If starting from the 17th, the three ensembles can reproduce the PV cut-off from the large scale at the right timing (not shown) probably due to initial conditions being closer to the tropical-like conditions. When looking at the ensemble performance, a more in-depth analysis is carried out using the divergence (s^{-1}), vorticity (s^{-1}), and time tendencies
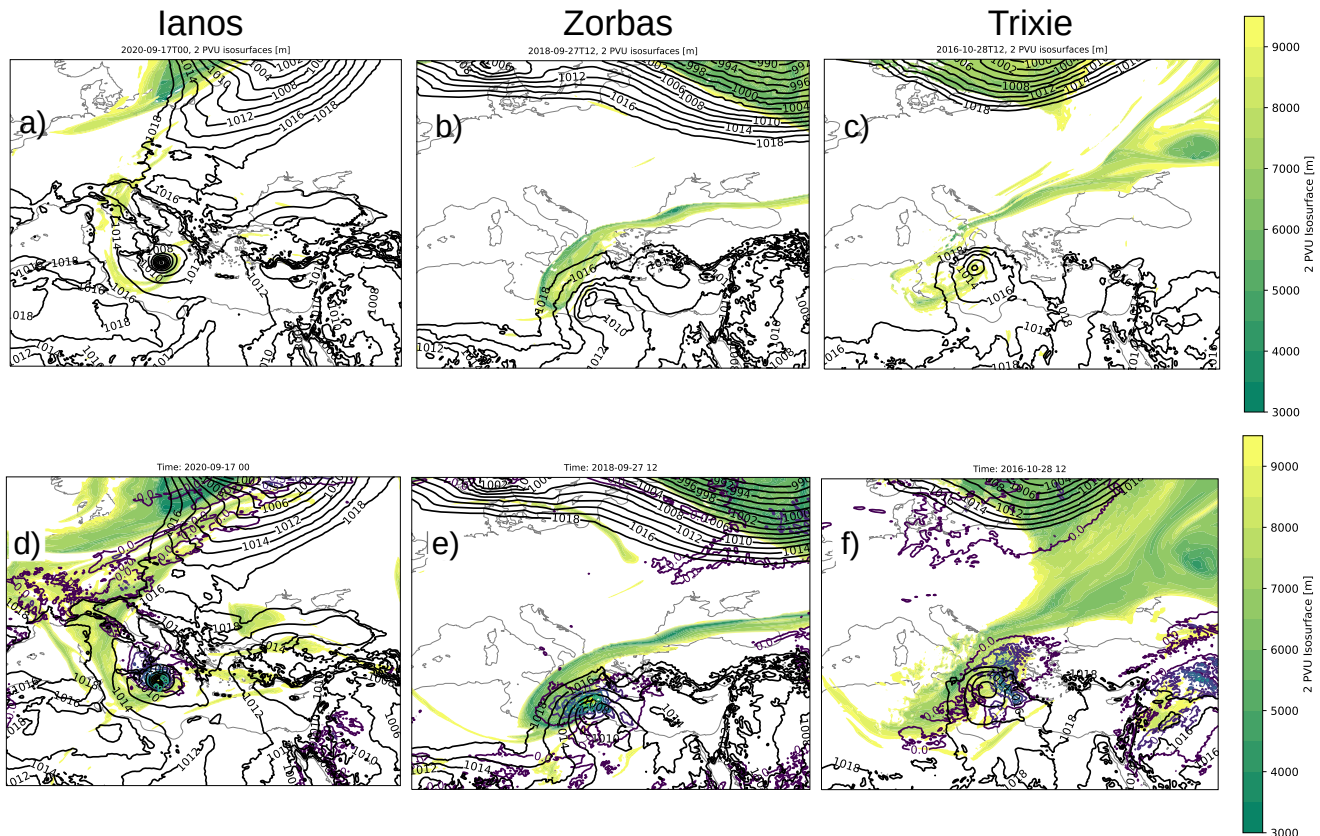
Figure 7. Height of the 2 PVU (PVU = $m^2 K kg^{-1} s^{-1} 10^{-6}$) isosurfaces together with the mean sea level pressure (black lines) in the operational analysis. For Ianos the 17th at 00 UTC is reported in Fig. (a) in the operational analysis and in (d) for the SPP-Conv ensemble experiment ensemble mean, for Zorbas the 27th at 12 UTC is reported in Fig. (b) in the operational analysis and in (e) for the SPP-Conv ensemble experiment ensemble mean and for Trixie the 28th at 12 UTC is reported in Fig. (c) in the operational analysis and in (f) for the SPP-Conv ensemble experiment ensemble mean. For Ianos the reported Fig. (d) is from the ensemble starting from the 17th, for Zorbas the reported Fig. (e) is from the ensemble starting from the 26th and for Trixie the reported Fig. (f) is from the ensemble starting from the 26th.

of the temperature (K/s) and specific humidity ($g/kg/s$) profiles around the cyclone centre (within a radius of 200 km). The
455   latter profiles are reported in Fig. 8 to 10 for the SPP-Conv experiment and in there the temperature and humidity tendency are
reported as Q1 and Q2 for temperature and humidity respectively, as is usual in the literature (Grabowski et al., 1999; Yanai
et al., 1973), where $Q1 = \frac{dT}{dt}$ and $Q2 = -\frac{L_v}{c_P}\frac{dq}{dt}$, with Q1 representing the heating in Fig. 7. In the case of Ianos, which be-
comes a warm core cyclone on the 17th of September (Fig. 8c and d at 00 UTC), the Q1 signals that the warming is happening
at 500 hPa and it has deepened from 12 hours earlier, on the 16th of September (Fig. 8a at 12 UTC), where the maximum is
460   located at 600 hPa. For Zorbas, the PV streamer is evident and it is occurring one day prior to the tropical phase (Fig. 7b) thus
inducing an intensification of the cyclone. This is well reproduced by the SPP-Conv ensemble experiment shown in Fig. 7e, as
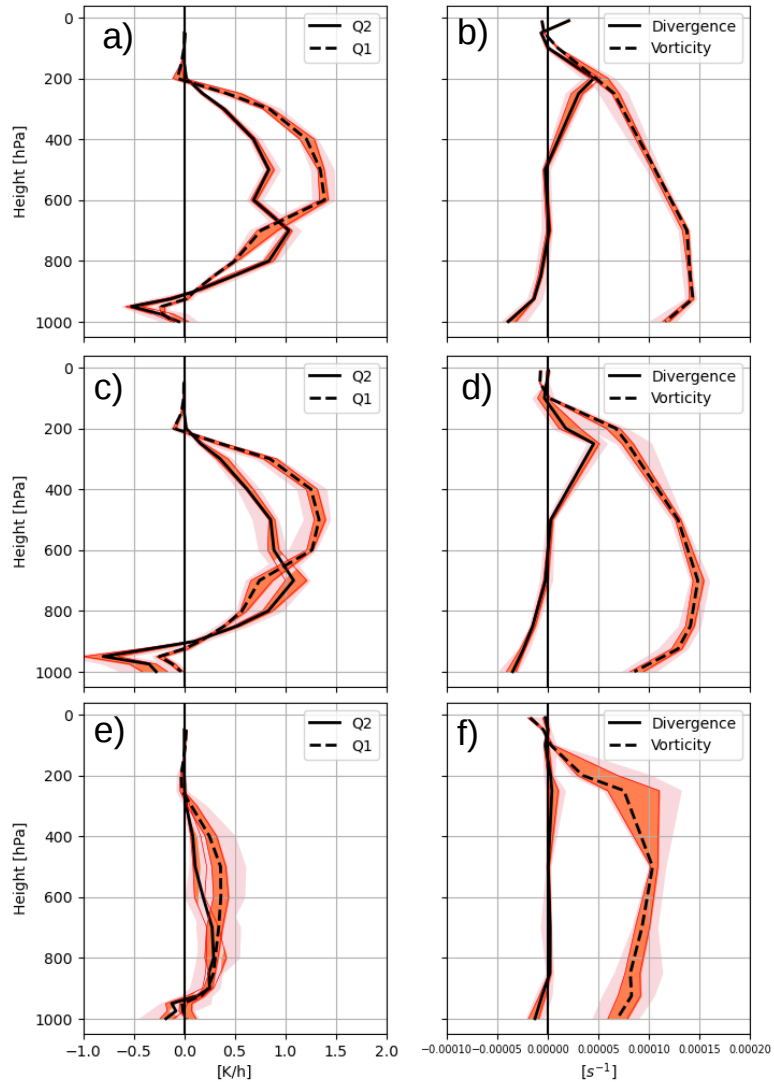
Figure 8. Analysis of the intensification and transition to tropical-like characteristics for Ianos as represented by the SPP-Conv experiment. The $Q1 = \frac{dT}{dt}$ and $Q2 = -\frac{L_v}{c_P}\frac{dq}{dt}$ profiles are shown in the first column and the vorticity and divergence profiles are shown in the second column. Fig. (a) and (b) are taken on the 16th of September at 1200 UTC. Fig. (c) and (d) are taken on the 17th of September at 00 UTC. Fig. (e) and (f) are taken on the 20th of September at 12 UTC. These profiles belong to the simulation starting on the 16th. The colours shading is the same of Fig. 4.

well as for the other two ensemble simulations INI and SPP (not shown). The values of the height of the 2 PVU isosurfaces coincide between the operational analysis (in Fig. 7a to c) and the ensemble simulations (in Fig. 7d to f). Similar behaviour to the one seen in Ianos, regarding the heating, can be observed for Zorbas in Fig. 9a and b. On the 27th of September at 12 UTC

465 the heating is below 600 hPa even if there is already a weak divergence over 600, underlining the presence of a still shallow vortex. Once again the PV-cutoff will happen 12 hours later when Zorbas will also reach the maximum intensity as indicated by Fig. 4 where a similar delay of 12 hours is present.
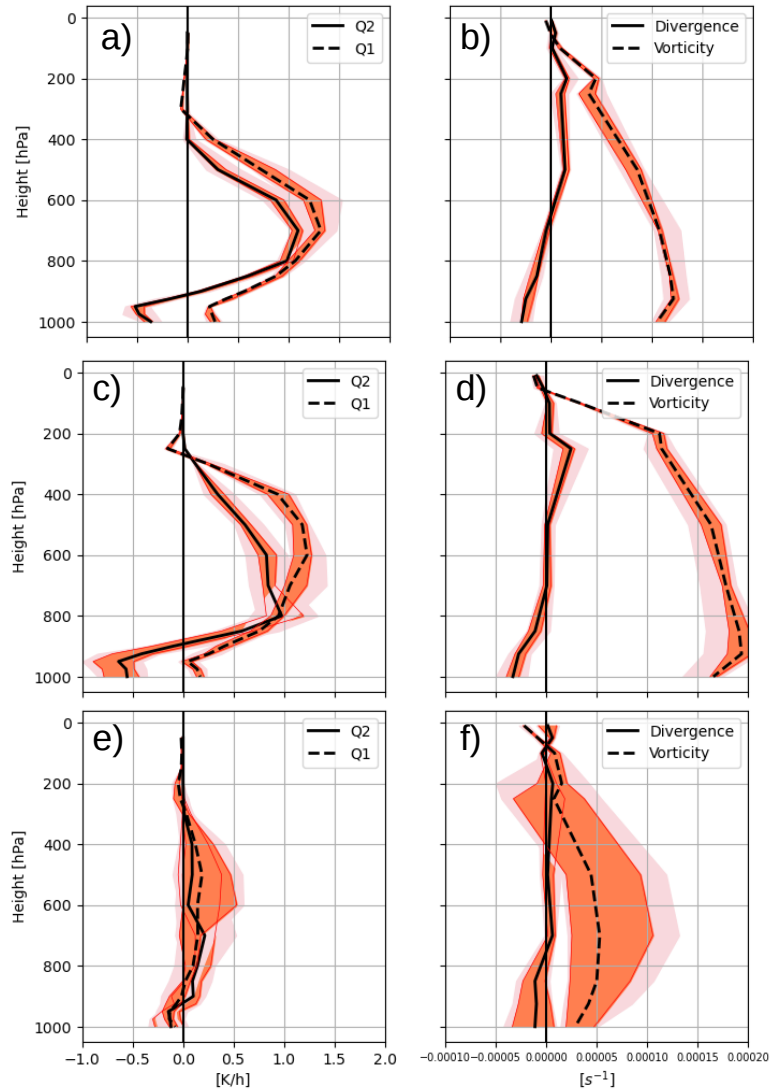
Figure 9. Same as Fig. 8 but for Zorbas. Fig. (a) and (b) are taken on the 27 September at 1200 UTC. Fig. (c) and (d) are taken on the 28 September at 1200 UTC. Fig. (e) and (f) are taken on the 1st of October at 1200 UTC. These profiles belong to the simulation starting on the 27th. The colours shading is the same of Fig. 4.

In the case of Trixie, even if the PV anomaly is well reproduced by the SPP-Conv ensemble, compared to the analysis, the convective heating, reported in Fig. 7f, is not aligned with the PV streamer. This happens in the time step where the cyclone is intensifying before dying out in the ensemble simulations (between 28 and 29 October). When looking at the vertical profiles in Fig. 10a and b, one day prior to 28 October, little warming (low values of Q1 and Q2 in the mid-troposphere) and low convergence in the lower troposphere can be noticed, lower values compared to the other two cyclones, nonetheless signaling a brief intensification phase for the cyclones. Indeed, when comparing these results with the minimum core pressure reported in Fig. 4 one can say that Trixie's initial state is well captured by the ensemble starting on the 27th leading to the first cyclone intensification of the 28th. However, if looking at the ensemble mean of the other starting dates, in particular the 25th , the PV streamer and the surface vortex are even more misaligned. Indeed, with the forecast starting date closer to the event, the alignment between the convective heating and the PV streamer is better reproduced (see Supplementary Fig. S6) which also leads to a better reproduction of the cyclone intensity.

Furthermore, while for Ianos and Zorbas, the presence of the cut-off low is well simulated by the ensemble experiments compared to the analysis (Supplementary Figs. S3 and S4), this is not the case for Trixie. In the ensemble simulations of Trixie, the cut-off low disappears after the 29th (Supplementary Fig. S5 shows the different reproduction of the presence of the cut-off low and how it changes with different starting dates). Its position and intensity had an influence on the track and intensity of Trixie, in accordance with what was suggested in the literature (Pytharoulis et al., 2000). Indeed, in the analysis, two distinct lows are formed separately (Supplementary Fig. S3) and the first to form is the one responsible for the Trixie surface vortex, by bringing instability from the upper troposphere to the lower troposphere. In the ensembles, this separation is not well captured. The formation of the second cut-off low prevails and the first one is weakened (Supplementary Fig. S4), influencing the development of Trixie after its formation, as will be discussed in the following section.

5.2 Cyclones Intensification

As underlined in the literature the factor that contributes to the development and intensification to reach a tropical-like state for Mediterranean cyclones is the pairing of the upper-level instability with the lower-level one (Flaounas et al., 2022). More specifically, Carrió et al. (2017) highlights the importance of the upper-level dynamics in intensifying the surface vortex and supporting the tropical transition of the cyclone. This is shown in Fig. 11, which represents the potential vorticity field and the meridional and zonal winds in a cross-section of latitude and pressure, at different stages for each medicane for the operational analysis. There, in Fig. 11 a, d, and g, the PV field is shown for the 24 hours before the cyclone became tropical-like and it is shown that there is an anomaly of the potential vorticity in the lower troposphere, around 800 hPa, which is a signal for the formation of a surface vortex for all the cyclones accompanied by a production of PV by diabatic processes. In Flaounas et al. (2022), it is summarized that the processes that can underlie the lower-level PV maxima can be the surface fluxes and the release of latent heat due to the organization of strong convective activity. In the upper troposphere, a PV anomaly develops and penetrates from the stratosphere. This happens around the position of the cyclone. After 12 hours (Fig. 11b, e, and h) the two PV anomalies, the upper and the lower, start to align. The same mechanism has been recognized in the literature by Cioni
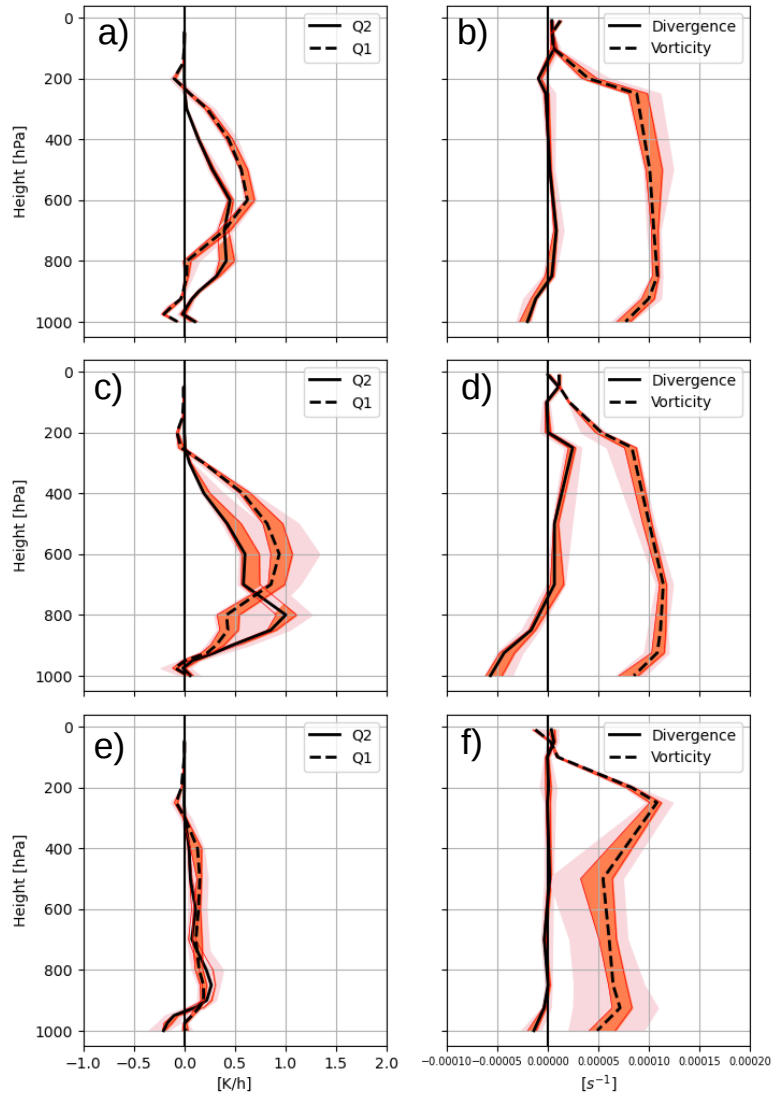
Figure 10. Same as Fig. 8 but for Trixie. Fig. (a) and (b) are taken on the 27 October at 1200 UTC. Fig. (c) and (d) are taken on the 28 October at 0000 UTC. Fig. (e) and (f) are taken on the 30 October at 1200 UTC. These profiles belong to the simulation starting on the 27th. The colours shading is the same of Fig. 4.

et al. (2018) and Miglietta et al. (2017). Finally, the tropical phase is reached when a cyclonic wind circulation completely surrounds the PV anomaly (Fig. 11c, f and i), the so-called "PV-tower". This is the case for all three cyclones. However, for Zorbas and Trixie deep, convective activity is higher during the intensification phase of the cyclone and then decreases as the maximum intensity is reached, as also recognized by Dafis et al. (2020). This can be seen in the cross-sections reported in Fig. 11 where the lower level PV anomaly is larger in the earlier stages before maximum intensity in Zorbas and Trixie (Fig. 11e

505
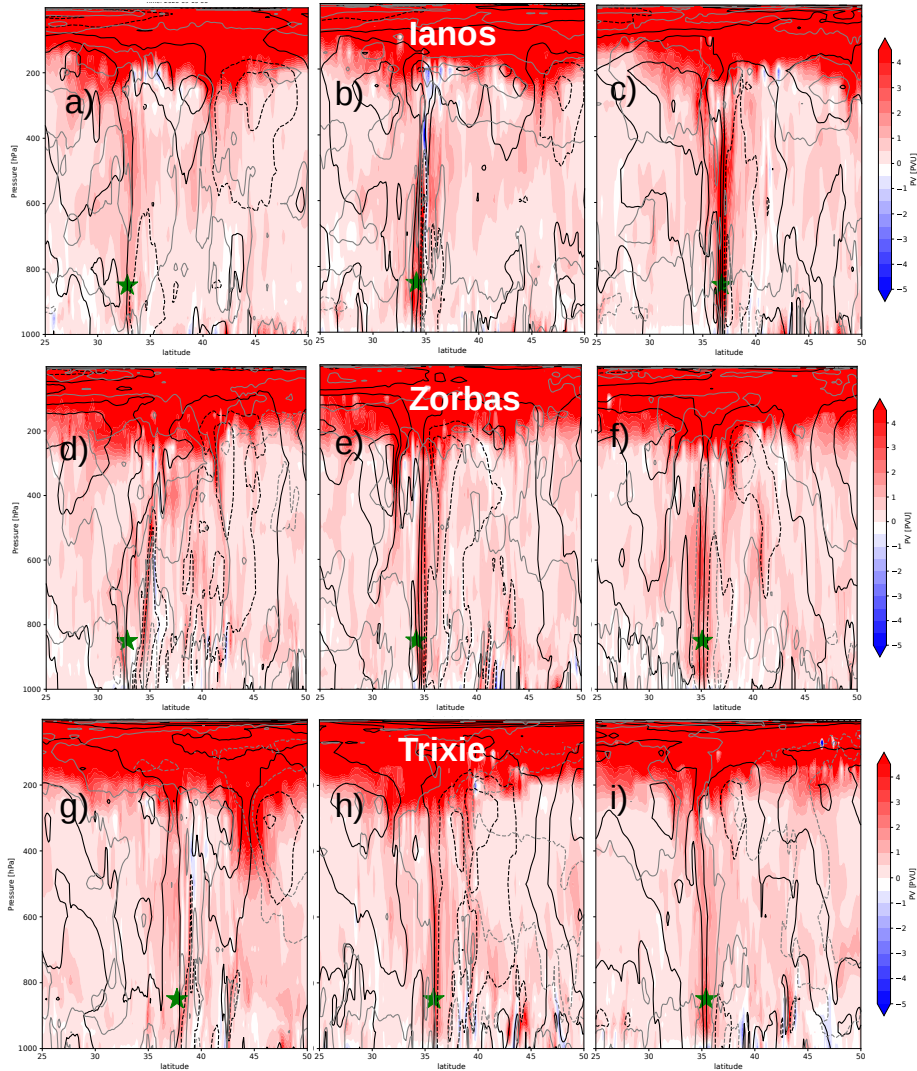
Figure 11. Cross section of the operational analysis potential vorticity field cross-section at latitudes from 25° to 50° and pressure taken in ⟶ at the longitude of the cyclone's central minimum pressure of the cyclones (green star). The PV is in colour and the black lines represent the zonal wind, while the grey lines represent the meridional wind. For Ianos the cross sections shown are for the 16th at 00 UTC, the 16th at 12 UTC and the 17th at 00 UTC in Fig. (a), (b) and (c) respectively. For Zorbas the cross sections belong to the 27th at 12 UTC, the 28th at 00 UTC and the 28th at 12 UTC in Fig. (d), (e) and (f) respectively. For Trixie the cross sections belong to the 29h at 00 UTC, the 29th at 12 UTC and the 30th at 00 UTC in Fig. (g), (h) and (i) respectively.

and h) compared to Ianos (Fig. 11b). It should be noted that the generation of the diabatic PV anomaly in the lower and middle

troposphere is relevant. In fact, as also shown in the previous section, the alignment of the convective heating (taken at 500 hPa in Fig. 7d to f) and the PV anomaly is necessary for the intensification of the cyclones.

For Ianos, the tropical-like phase on the 17th of September is reproduced, with the INI experiment showing a slightly weaker PV than the SPP-Conv ensemble mean (for the simulation starting from the 16th shown in the Fig. 12a and b). The tropical-like phase is accompanied by strong divergence above 400 hPa and convergence below 800 hPa (Fig. 8b and d) and by an increase of diabatic heating (Q2 profile) due to condensation. Vorticity increases in the middle and upper troposphere on 17 September (Fig. 8d) compared to the 12 hours before. The warm core is sustained for another day and the cyclone begins to dissipate around 19 September. By the 20th of September (Fig. 8e and f) the cyclone is dying out, with almost no divergence and no convective heating. Comparing Fig. 8c, Fig. 9c and Fig. 10c it can be said that the spread is smaller for Ianos, which means less uncertainty about the nature of the medicane compared to Trixie and Zorbas. Moreover, in the case of Ianos, these results compare well with the precipitation field shown in Fig. 5, which is the best simulated among the three medicanes, at least regarding the simulations starting on the 17th. In addition, as mentioned in the analysis of the Hart parameters for Ianos, the presence of a deep warm core is well simulated with decreasing spread and error with starting dates closer to the event (Fig. 6a to d), correlating with the better reproduction of the PV-tower generation. The comparison between the SPP-Conv and the INI ensemble shows that the former experiment produced a slightly more intense cyclone than the analysis and the latter experiment, probably due to the effects of the convective parameterization perturbation.

For Zorbas, on the 28th of September, the PV values in the two ensemble experiments were higher than the analysis, signaling a slightly more symmetric and intense cyclone (Fig. 12c and d), also in agreement with the results for the Hart parameters shown in Fig. 6e to h. However, the two experiment ensemble means (INI and SPP) are very similar and they both represent the actual presence of a PV-tower. Looking at Zorbas vertical profiles in Fig. 9, it can be seen that the divergence increases above 400 hPa in the tropical phase, around 28th September (Fig. 9d at 12 UTC) compared to the previous day (Fig. 9a and b on the 27th September at 12 UTC). The same is true for the vorticity in the upper and middle troposphere. The warming intensifies and moves into the upper troposphere (Q1 and Q2 profiles in Fig. 9a and c). After two days of "tropicalization" the cyclones begin to weaken and by the 1st of October (Fig. 9e and f) the divergence is almost null and the warming decreases. These results obtained for Ianos and Zorbas are similar to those obtained for tropical cyclones (Geetha and Balachandran, 2016; Lin and Qian, 2019) where intensification occurs. Therefore, it can be said that Ianos and Zorbas go through a tropical phase in the ensemble experiments. There, the heating observed in the simulation is caused by the release of latent heat in the condensation process inside the clouds, as also confirmed by observations for Ianos (Zimbo et al., 2022; Lagouvardos et al., 2022). Indeed, heat fluxes from the sea surface often trigger convection and support intense and persistent diabatic warming through latent heat release from condensation (Carrió et al., 2017). As shown below, the surface fluxes played a role in the intense phase of both Zorbas and Ianos. The spread in Zorbas is reduced by the forecast start date closer to the event (not shown) in favour of the higher values for Q1 and Q2 (shown in Fig. 9c which represents the profiles of the latest start date) which justifies the results for the Hart parameters in Fig. 6e to h. Here, the spread of the upper-level thermal wind is reduced and the error decreases.

Trixie, on the other hand, does not present enough strong surface vortex to match the PV anomaly in the upper level for
545 both experiments (Fig. 12e and f) starting on the 25th. Looking at the other starting dates simulations, there appears to be a
stronger lower-level instability (not shown). However, this cannot be sustained by the simulation. For Trixie indeed, the deep
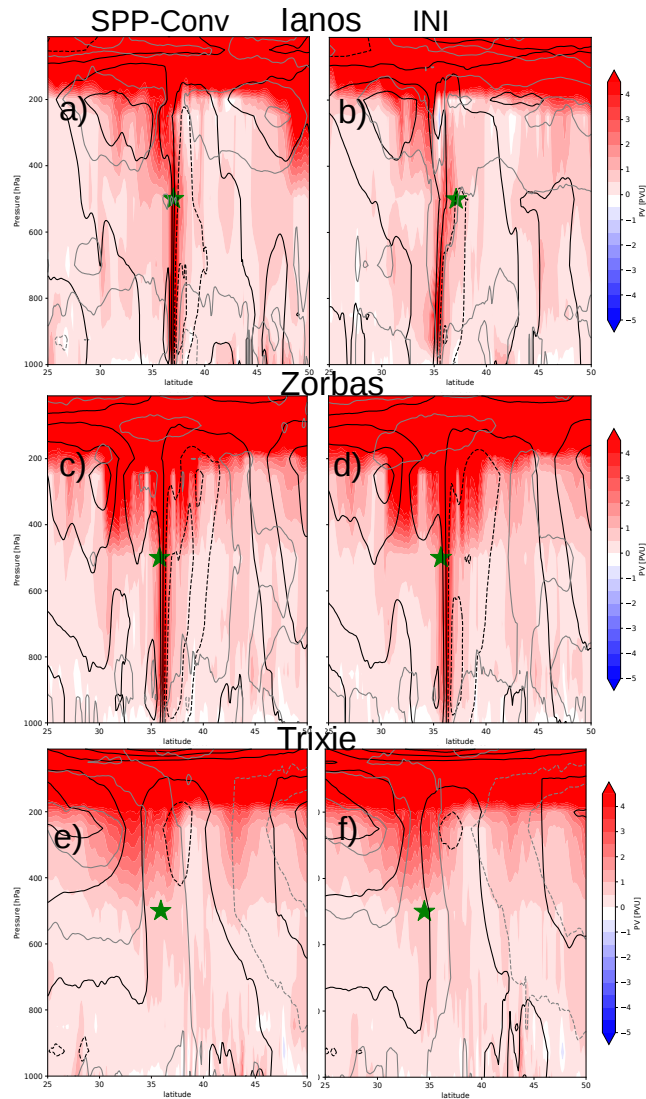
Figure 12. Potential vorticity field cross-section in latitude from $25°$ to $50°$ and pressure taken in the longitude of the central minimum
pressure of the cyclones (green star) as represented by the SPP-Conv and the INI ensemble means in the first and second column respectively.
The PV is in colour and the black lines represent the zonal wind, while the gray lines represent the meridional wind. For Ianos the cross
sections shown regard the 17th at 00 UTC in Fig. (a) and (b). For Zorbas the cross sections belong to the 28th at 12 UTC in Fig. (c) and (d).
For Trixie the 30th at 00 UTC is shown in Fig. (e) and (f) respectively.

warm core state is never reached. As said before this cyclone is the weakest and it can intensify only on the 28th of October in the ensemble simulations (Fig. 10c and d at 00 UTC). The convective heating represented by a positive Q1 and Q2 is weaker compared to the other cyclones (Fig. 8 and 9) and the maximum is located in the mid-troposphere, signaling a shallow warm core. The divergence, which is increasing compared to the previous 12 hours (Fig. 10b and d) is not accompanied by an increase in vorticity and it starts at mid-troposphere. The warming is weak and there is no divergence (Fig. 10e and f). Trixie presents the highest spread regarding the warming, also mirroring the results from the Hart parameters reported in Fig. 6i to n. The warming, which does not correspond to a shallow warm core, is reached only on the 28th of October but is absent on the 30th of October, when Trixie is supposed to become a tropical-like cyclone (Dafis et al., 2020). Thus the Hart parameters values are justified by the absence of upper-level warming for Trixie. This is also correlated with the minimum core pressure development presented in Fig. 4 and for the accumulated precipitation in Fig. 5, where every ensemble experiment diverges from the analysis and observations after the 29th of October. These results indicate that Ianos and Zorbas are simulated mostly with the right tropical-like phase, with almost the right timing (12 to 24 hr of delay as mentioned above), while the ensemble simulation for Trixie fails to reproduce the right intensification of the cyclone, simulating a shallow warm core on the 28th and missing the deepening on the 30th.

The ensembles appear to have been able to better reproduce the large-scale upper-level dynamics, but there seem to have been issues in reproducing the presence or absence of PV anomalies generated by diabatic processes and the latter interaction with the upper-level one, specifically for Trixie. In order to understand this latter aspect, the convective activity in the three medicanes has first been analyzed by means of the Convective Available Potential Energy (CAPE). The main result is weaker convection indicated by a weaker CAPE in Trixie. Indeed in Fig. 13 there is a comparison between CAPE around the cyclone centre for Zorbas and Trixie at the intensification tropical-like state. In the ensembles, the reduced convective activity near the centre reported in Fig. 13 for Trixie underlines the lower energy conversion from diabatic heating. Such a situation can be ineffective in driving the cyclone to a state in which it is able to self-sustain by the wind-induced surface fluxes (Emanuel, 1986) and the transition to the tropical-like cyclone being degraded as already found in Koseki et al. (2021).

This is correlated with the effect of the surface fluxes, being much higher in the case of Zorbas and Ianos compared to Trixie (Supplementary Fig. S7). Indeed, also the total heat flux at the surface (the sum of the sensible and latent heat flux) has been inspected. In Supplementary Fig. S7 is made clear that in the ensembles for Ianos and Zorbas the surface fluxes amount to around 500 W/m^2 and are concentrated for Ianos around the centre and for Zorbas are much more spread out. For Trixie, instead, the values are much lower and not at all comparable with the other cyclones. In general, by the 29th of October, in the Trixie simulation, the convection is weakening and by the 30th is absent in the ensemble experiments, compared to the analysis. Thus, this reduced CAPE in the ensemble simulations is signaling a simulated weaker low-level vortex and a lower PV anomaly.

The surface level production of PV in Trixie is not enough to match with the upper tropospheric high PV field as reported in Fig. 12e and f, or they are not in phase. In the ensemble simulations starting on the 27th, the amount of diabatically generated
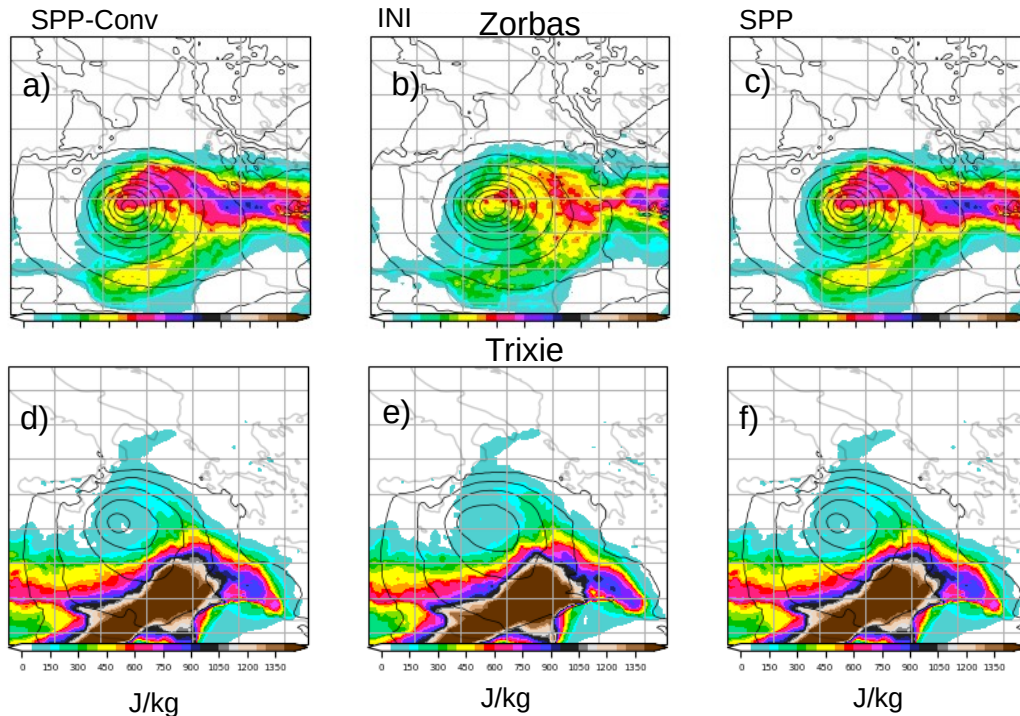
Figure 13. Convective Available Potential Energy (J/kg) (in colours) and mean sea level pressure (in lines) for the three ensemble experiments ensemble means. For Zorbas the 28th at 12 UTC is shown in Fig. (a), (b) and (c) for the simulation starting from the 27th. For Trixie the 28th at 12 UTC is shown in Fig. (d) (e) and (f) for the simulation starting from the 27th.

PV comparable to the analysis is not able to align with the upper-level one, even though the alignment is better captured with starting dates closer to occurrence (Supplementary Fig. S6). This pertains to both the INI and SPP experiments, as mentioned before, meaning that the production of the right diabatic processes is equally sensitive to initial conditions and to physical and

585   more specifically convective processes. The analysis points out that the cyclone dies before the 30th of October, due to the low-level vortex being too weak and not able to interact properly with the upper-level disturbances. Actually, the surface vortex disappears with the weakening of the upper-level cut-off low, and due to the absence of a reinforcement of the lower level PV production by the upper level one, meaning erosion of PV by the presence of intense diabatic processes, as for instance is happening in Zorbas (Portmann et al., 2020). Firstly, as mentioned in the previous Section, in the ensemble simulations of

590   Trixie (both INI and SPP), the cut-off low that was crucial for the formation of the surface cyclone, disappears after the 29th and the formation of the second cut-off low weakens the first. With the weakening of the cut-off low, Trixie starts lowering its intensity. Only a few members can follow the weak cut-off low (Supplementary Fig. S3). This has had an impact on the simulation of the already weak cyclone, Trixie. Indeed, it is hypothesized that Trixie is formed as a lower-level vortex mainly due to the thermodynamic disequilibrium generated by the upper-level cut-off low. If the latter is not well simulated, being weaker,

595   it is not able to sustain the surface vortex. Secondly, when the surface level vortex is better reproduced, the misalignment with

the upper-level PV anomaly does not permit reinforcement of the convection. Homar et al. (2003); Cioni et al. (2018) showed that the upper-level PV structure indirectly acts on the cyclone deepening through a modification of the surface circulation.

As mentioned above, the simulation of strong convective activity seems to be important in all three cyclones, which is associated with latent heat release, developing in the central region of the cyclones (Fig. 8, 9 and 10). As recognized in the literature, either the surface fluxes or convective activity can predominate in the intensification of the surface level vortex, as identified for different medicanes (Davolio et al., 2009; Miglietta et al., 2017; Chaboureau et al., 2012; Fita and Flaounas, 2018). While surface fluxes seem to have also played a role in the intensification of both Ianos and Zorbas (Supplementary Fig. S7), in the case of Trixie specifically deep moist convection seems to be the main mechanism leading to the maintenance and deepening of the system, as due to the interaction of convection with the upward forcing induced by the PV streamer (Chaboureau et al., 2012). Indeed, for Trixie is the long-lasting deep convective activity that may have played an important role in their intensification later than their genesis time, as also recognized by Dafis et al. (2020), and its weakening or even absence compromises the forecast, as happens in the presented ensemble experiments. While the tracking is mainly influenced by the position of the cutoff low and the PV steamer position, the simulation intensification phase and timing are dependent on how the convection is reproduced and interacts with the upper-level PV structure.

5.3 The role of the Sea Surface Temperature

By looking at the Sea Surface Temperature (SST) anomaly, it is found that it is higher for Zorbas (Ianos is once again similarly affected by the SST anomaly as Zorbas) upon formation compared to Trixie, as reported in Fig. 14 which represents the ensemble mean anomaly of the SPP-Conv and INI experiments for Zorbas and Trixie for comparison. On one hand, for Zorbas (Fig. 14a b and c) the SST is anomalously high compared to the climatological SST of September (obtained by using the ERA5 reanalysis SSTs over the Mediterranean Basin from 1991 to 2020), of on average 2° C. On the other hand for Trixie, the anomaly (with respect to the climatological SST of October) decreases, and in the area of cyclone formation is very weak compared to Zorbas (Fig. 14d, e and f). This means that the air-sea temperature contrast did not play a crucial role in Trixie generation and maintenance as it did for Ianos and Zorbas, probably resulting in weaker low-level vortex altogether (mirroring what is shown in Supplementary Fig. S7 for the surface fluxes).

Indeed, the ensemble experiments results compare fairly well to the operational analysis for the SST anomaly for the three medicanes (not shown), underlining the relative importance of the air-sea interaction in the tropicalization of certain Mediterranean cyclones. Noyelle et al. (2019) found that the SST state has a strong influence on the medicanes intensities and that increased SSTs lead to greater probabilities of tropical transitions, stronger upper-level warm cores and lower pressure minimum pressure, by influencing the intensity of fluxes from the sea, which leads to greater convective activity before the storms reach their maturity. The higher surface temperatures in Ianos and Zorbas help feed the medicane the moisture, through surface fluxes (Pytharoulis, 2018), allowing the convection to develop more effectively (Koseki et al., 2021; Cioni et al., 2018).
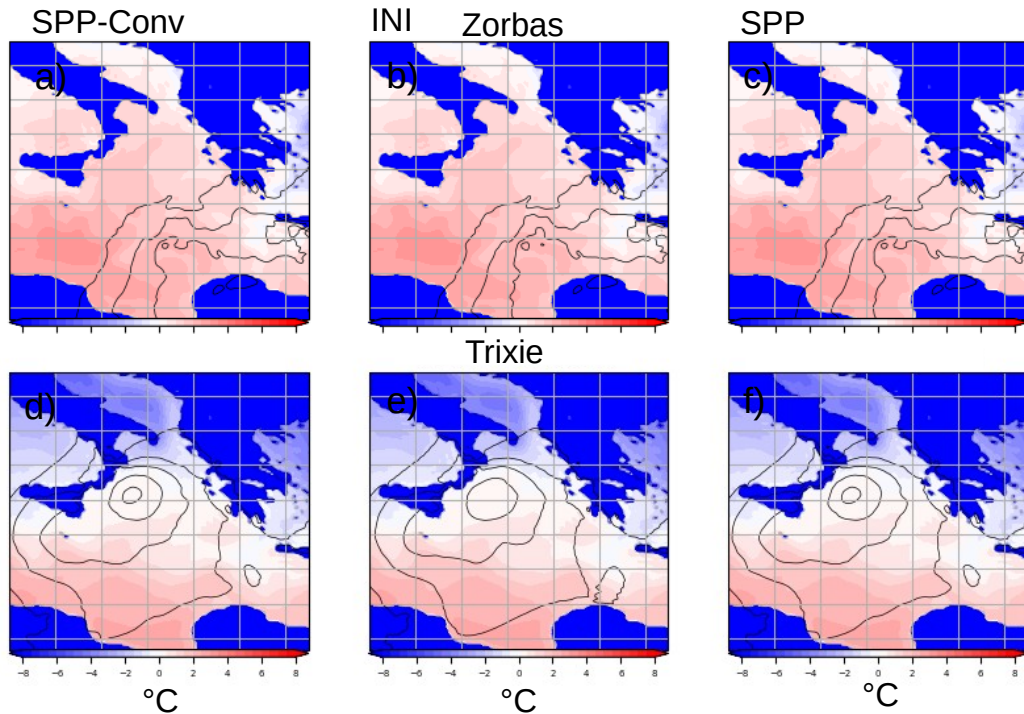
Figure 14. Sea Surface Temperature anomaly (°C) (in colours) and mean sea level pressure (in lines) for the three ensemble experiments ensemble means. For Zorbas the 27th at 00 UTC is shown in Fig. (a), (b) and (c) for the simulation starting from the 27th. For Trixie the 28th at 00 UTC is shown in Fig. (d) (e) and (f) for the simulation starting from the 27th.

6 Discussion and Conclusion

Predicting and simulating medicanes is a difficult task due to them being extreme events found near the tail of the forecast dis-
630   tribution (Majumdar and Torn, 2014) and due to the complexity of the processes involved. The specific barriers to predictability and the atmospheric conditions that lead to the formation and evolution of medicanes are not fully understood. Research using multi-physics approaches has found that the track, intensity, and duration of medicanes are heavily sensitive to factors such as convection, microphysics, and boundary-layer parameterizations (Ragone et al., 2018; Miglietta et al., 2015). Indeed, this study is one of the first steps toward understanding this sensitivity by using ensemble forecast simulation.

635

The analysis was focused on three medicanes using the ECMWF model IFS ensemble forecast system. In addition to the op-
erational ensemble forecast, the TOT ensemble, some other experiments have been carried out, the initial condition perturbation ensemble, INI, and two ensembles with SPP, in one case perturbing only the parameters of the convection parameterization, SPP-Conv, and in the other perturbing the parameters of all relevant physical parameterizations, SPP. The approach used was
640   aimed at analyzing the tracks, intensity, i.e. central pressure, precipitation, and parameters characterizing the thermal structure

of the cyclones. Secondly, the processes behind the generation and development of the cyclones have been analyzed in conjunction with the previous analysis.

The result of this study, compared to previous ones (Di Muzio et al., 2019; Chaboureau et al., 2012; Pantillon et al., 2013), which used only the operation ensemble forecast of ECMWF, points out the benefit of using the Stochastically Perturbed Parameterization, SPP ensemble forecast compared to just perturbing the initial conditions. The use of SPP, and in particular the perturbation of convective parameters (SPP-Conv), was found to compare well with the INI and TOT experiments in terms of tracking, cyclone intensity and precipitation. Similar results have been obtained in Ollinaho et al. (2017), especially regarding precipitation. The experiments are usually underdispersive in terms of tracking position, although the TOT experiment gives better results. Indeed, the ensemble forecast TOT has proven to be the best in terms of spread and error compared to the tracking, intensity and precipitation of cyclones. This is due to the inclusion of the model's physics perturbation, in line with what was found in Lang et al. (2021). The ensemble spread and mean are generally lower in the SPP experiments. For instance, the analysis of the thermal structure and symmetry shows that for the upper-level thermal wind, the smaller spread is obtained in most cases in the SPP-Conv experiment (in particular at later forecasts). Nonetheless, the two SPP ensembles are able to produce the same spread as the initial condition perturbation experiment at later time steps, highlighting the benefit of introducing physical parameters perturbations, especially with respect to convection, compared to use only perturbations of the initial conditions (Lang et al., 2012; Ollinaho et al., 2017). Moreover, the similarity of the SPP and the SPP-Conv results, especially for the thermal structure and thermal asymmetry, highlights that the uncertainties linked to the convection parameterization are predominant in the simulation of these types of phenomena, confirming previous results (Pytharoulis, 2018; Fink et al., 2012; Wimmer et al., 2022). Finally, with respect to the above-mentioned cyclone characteristics, it is found that there is a common gradual decrease in the error with the forecast starting date closer to the occurrence. This is consistent for all three ensemble experiments and it is specific for Ianos and Zorbas. For Trixie this decrease in the error is weaker and, in some cases, non-existent. Indeed, as pointed out in the results the simulation of this particular cyclone can be considered as a missed forecast (as shown by the track in Fig. 1 and the intensity in Fig. 4).

Specifically, regarding the reproduction of the minimum central pressure by the ensemble forecasts (Fig. 4) there is generally a time shift in the reproduction of the minimum intensity, where both the Ianos and Zorbas ensemble means reach the maximum intensity with a delay. Since the delay decreases as the forecast starting date gets closer to the event, this is due to the improved initial conditions. Indeed, it is found that the maximum intensity is reached when the upper-level PV streamer and the surface-level vortex are aligned, and the latter is better captured by starting the simulation closer to the cyclone's onset. This is consistent with what was found in Flaounas et al. (2015) where they underlined that the intensity of the surface cyclone increases while the streamer is on the western side of the cyclone and begins to decrease as the streamer is wrapping over its centre. It is noteworthy that for Zorbas the intense phase (i.e. low values of minimum core pressure) is maintained for a longer period, compared to the operational analysis, as underlined by the minimum core pressure trend in Fig. 4, and by the PV tower reported in Fig. 12. This is probably due to the fact that most members (especially regarding the SPP ensembles) spend

most of their lives at sea and do not cross land over Greece, thus managing to sustain themselves for a longer period through condensational heating and air-sea interaction.

Then, by looking at the simulated precipitation distribution, compared to the GPM-IMERG satellite observations, it is shown that only for Ianos, the precipitation field is well reproduced by the ensembles, with the SPP experiment being slightly more intense than the others. Even if the GPM-IMERG dataset tends to overestimate the precipitation over the Mediterranean (Peinó et al., 2022; Caracciolo et al., 2018), the simulated precipitation for Zorbas and Trixie is too weak. However, it is discussed that in general, the precipitation maximum compares better with the forecasts starting date closer to the occurrence, thus for Zorbas, starting the ensemble forecasts on the 28th would have shown better-simulated precipitation. It could be argued that a finer resolution than a 9 km resolution would improve the reproduction of the intensity and track of the tropical-like Mediterranean cyclones. A recent single forecast experimental tropical cyclone simulations at 4 km resolution by (Majumdar et al., 2023) reveal that the 4 km simulations produce deeper and more realistic tropical cyclones in terms of radial wind structure compared to the observations than the 9 km forecasts. However, in the aforementioned work done within the DestinE project (Gascón et al., 2023), preliminary simulations carried out with IFS at 4 km resolution did not show any significant changes in the simulated tracks and intensity of Medicanes, except for slightly more intense winds. This applies to both Trixie (https://confluence.ecmwf.int/x/soQvEQ) and Ianos (https://confluence.ecmwf.int/x/soQvEQ) where the 9 and 4 km resolution simulations are roughly equivalent.

It is shown that for Ianos and Zorbas the forecasts are accurate at reproducing both the thermal structure and symmetry of the cyclones, compared to the analysis value. The only exception to the reasonable reproduction of the storm thermal structure is the upper-level thermal wind in Trixie (Fig. 6a-c-e). This means that for Trixie, where the analysis value reported the presence of a warm core ($-V_T^U = 25$ in Table 2), the three ensemble forecast presents a cold core cyclone (negative $-V_T^U$ values). This, together with the underestimation of the deepening of the cyclone, can explain the simulated precipitation being weaker than the observations since the simulated cyclone is not able to reach the warm core, thus the convective heating is lower affecting the simulation of the precipitation. From the Q1 and Q2 profiles, it is evinced that the cyclone seems to intensify around the 28th and to die out by the 30th, when it should have entered the tropical phase, as mentioned in Dafis et al. (2020).

Indeed, through tracking, it was verified that with regard to the Trixie simulation, there is a southeastward shift of the trajectory with respect to the analysis (Fig. 1). A lower spread in the tracked position was found for Zorbas and Ianos compared to Trixie, but the error of Trixie exceeds 800 km. This is attributable to the fact that the ensemble forecast starts too early with respect to the cyclone intensification phase for Trixie. This result, in particular, aligns with previous studies that had pointed to Trixie's low occurrence probability up to two days earlier (Di Muzio et al., 2019). Indeed, There is an inherently low probability of medicanes occurrence (as seen in Di Muzio et al. (2019)) and the development of a warm core cyclone depends on many factors, large-scale factors and surface fluxes, that can be improved by the initial conditions of a preexisting cyclone.

In order to evaluate the obtained results, an investigation of the development processes and their simulation were linked to the forecasts track position and intensification of each cyclone. First, it has been pointed out that Ianos, Zorbas, and Trixie all require the presence of a PV streamer together with a deep cut-off low in order to form. This underlines the nature of these cyclones as being born in a baroclinically unstable environment. This is initially reproduced reasonably well, although specifi-

715 cally in the case of Trixie, the ensembles may have started too early to capture the interaction between the two, making Trixie a weaker cyclone and ultimately leading to its ending. As pointed out in the previous section, the cut-off low which contributes to the development of Trixie quickly weakens in the ensemble simulations after the 29th and is then shut down in favour of another one that crossed the Ionian sea (Supplementary Fig. S4 and S5).

720 Then, it has been shown that after the formation of the three cyclones, the operational analysis represents a clear interaction between the surface level vortex and the PV anomaly in the upper troposphere in all three cases, the PV tower, in order for them to intensify and eventually reach "tropical-like" features (Carrió et al., 2017; Cioni et al., 2018; Flaounas et al., 2022). This is present in the ensembles (both for SPP and INI) in the case of Ianos and Zorbas, where, the upper-level PV anomaly brought by the PV streamer is able to match with the lower-level PV production by diabatic processes. As also pointed out,

725 this surface cyclone is sustained by convective heating release by condensation, with surface fluxes supporting the cyclone in the most intense phase along with convective activity (Supplementary Fig. S7). In the case of Ianos, the convective activity peaks during the moist intense phase, as underlined by the PV anomaly in the PV cross-section in Fig. 11, while in the case of Zorbas, convective activity is present also before the cyclone tropical like phase (as also underlined by the PV anomaly in Fig. 11). The ensemble simulated cyclones are sensitive to the positioning of the PV streamer, which, as observed in the literature,

730 has a clear impact on the simulation of the medicane. In the case of Zorbas, as noted in Portmann et al. (2020), a westward shift of the PV streamer leads on average to weaker cyclones, which can be observed in the ensemble mean of Zorbas in Fig. 4. The displacement of the PV streamer is linked to the alignment with the surface level and the consequent creation of a PV tower. Furthermore, the intensity of the PV anomalies, as well as the height reached by the 2 PVU isosurface, may have played a role in the cyclone's greater or lesser intensity. In fact, in the case of Ianos, it can be argued that the cyclone is more intense

735 in the ensembles compared to the analysis due to the higher simulated PV anomaly and deeper PV streamer. In other studies, also using the ECMWF ensemble forecasting system (Chaboureau et al., 2012), it was found that later forecasts are able to capture better the thermal structure of the medicanes, due to the lower uncertainty of the positioning of PV streamer connected to the generation of the medicane. In general, in our study is assessed that the earlier the starting date the greater the misalign-ment (or the worse positioning of the upper-level disturbance) between the lower and the upper PV production. This is true,

740 particularly in the case of Trixie, where on the simulation starting too early, on the 25th, the lower level PV production is absent, and for the simulation starting on the 26th and the 27th it is very weak and not able to be reinforced by the upper level one.

Trixie is also a weaker medicane compared to Ianos and Zorbas (the central minimum pressure of Trixie is lower than the other two cyclones, as reported in Table 2), influencing the simulations. In a recent study by (Panegrossi et al., 2023), while

745 Ianos and Zorbas have been recognized as two of the most intense medicanes, Trixie has been characterized as one of the

weakest, not even reaching the status of deep warm core, as established by looking at passive microwave measurements and products. Here, it has been shown firstly that the surface fluxes in the phase of tropicalization and intensification are lower than the other medicanes. Secondly, it is underlined that the SST anomaly in the case of Trixie was low both in the analysis and in the ensembles, yielding to a weaker cyclone, and lastly that Trixie tends to shut off when the cut-off low vanishes in the simulations and generally tends to follow the PV streamer position. This makes it subject to being more dependent on the simulation of large-scale processes. More specifically the lower level PV production present in the analysis in Fig. 11 is absent in the simulations in Fig. 12. Since the surface fluxes and the anomaly of SST do not play a role, this makes the convective instability brought by the cutoff low necessary to sustain the cyclone convection. The deep cut-off low absence in the simulations can be linked to the medicane missing development in the case of Trixie. This is supported by the findings of Fischer et al. (2017), who hypothesized that tropical cyclones intensification rate after tropical cyclogenesis, in environments of upper-tropospheric troughs, is closely linked to the structure and temporal evolution of the upper-level trough.

Going back to the medicane classification, the three medicanes seem to belong to different medicanes categories. Ianos and Zorbas seem to belong to the one in which baroclinicity is important only in the initial stage and positive feedback between the latent heat release and the air-sea interactions is behind their intensification through Flaounas et al. (2022). Trixie seems to belong to the one in which baroclinic instability plays an important role throughout the cyclone's lifetime and most of their intensification is due to convection (Fita and Flaounas, 2018). Thus, one of the outcomes of this study, is that the ensemble forecasting of ECMWF is likely able to better capture the tropical-like features of the first category of medicanes. The investigation of this will be the subject of further study, also considering a greater number of medicanes. This analysis also underlines the different sensitivity of the diabatic processes in the simulation of these medicanes, because it makes it clear that convective heating has played a major role in the intensification of the cyclones and when absent is linked to the disappearance of the cyclone itself, as in the case of Trixie.

To conclude, this study confirms that similar processes are at play in the development of Mediterranean tropical-like cyclones and the predictability of these cyclones is linked to not only the reproduction of the precursor events (namely the deep cut-off low) but also to the interaction of the upper-level dynamics with the lower-level one (namely the PV streamer and the lower level PV production), in a similar way. This work, as urged in the literature (Dafis et al., 2020; Pytharoulis, 2018) underlines the relative importance of the upper-tropospheric troughs and PV streamer interactions with the troposphere for medicanes not only in one specific case, as often done in the literature (Portmann et al., 2020; Chaboureau et al., 2012; Cioni et al., 2018), but extending the analysis at least to a few different cases.

Finally, as discussed in Flaounas et al. (2022) the representation of cloud adiabatic processes is often believed to be a source of forecast uncertainty but dominated by the one created by initial conditions. This study, by comparing ensemble forecasts with the account of initial condition perturbation only and of physical parameterization only, underlines that the uncertainty produced by both ensembles is actually similar.

Code and data availability. The output of the IFS ensemble forecasts and the operational analysis data are available on the MARS Archive at https://www.ecmwf.int/en/forecasts/dataset/ecmwf-research-experiments and the precipitation dataset GPM-IMERG used for validation is freely available on the NASA data archives at https://gpm.nasa.gov/data/imerg. The python codes used to produce the analysis are available at https://doi.org/10.5281/zenodo.7912957.

Author contributions. All authors contributed to the conceptualization of the research. P.B., M.S., and P.B.C. worked on the methodology. P.B. carried out the ensemble simulations. M.S. and L.S. carried out the analysis of the ensemble simulations and P.B.C. supervised all the research group work. M.S. and P.B. wrote the original draft. All authors have read, reviewed, edited, and agreed to the manuscript.

Competing interests. No competing interests are present

Acknowledgements. This research has been funded by the Italian Ministry of University and Research (MIUR) and the University of Perugia within the program *Dipartimenti di Eccellenza 2018-2022,*by the European Centre of Medium Range Weather Forecast (ECMWF), by the *Fondo Ricerca di Ateneo esercizio 2021: Cambiamenti climatici: consapevolezza impatto sociale, modelli scientifici e soluzioni tecnologiche* and by the *CIRIAF (Centro Interuniversitario di Ricerca sull'Inquinamento e sull'Ambiente "Mauro Felli") - SSTAM* with the research project *Modelli predittivi ad alta definizione per fenomeni meteoclimatici nell'ambiente mediterraneo*. This article is a contribution to the COST Action CA19109 "MedCyclones: European Network for Mediterranean Cyclones in weather and climate"; The authors are grateful to Simon Lang and Martin Leutbecher for developing and providing the experimental SPP configuration and want to acknowledge high-performance computing support from ECMWF Supercomputing HPC facilities.

References

Baker, L., Rudd, A., Migliorini, S., and Bannister, R.: Representation of model error in a convective-scale ensemble prediction system, Nonlinear Processes in Geophysics, 21, 19–39, 2014.

Bechtold, P., Köhler, M., Jung, T., Doblas-Reyes, F., Leutbecher, M., Rodwell, M. J., Vitart, F., and Balsamo, G.: Advances in simulating atmospheric variability with the ECMWF model: From synoptic to decadal time-scales, Quarterly Journal of the Royal Meteorological Society: A journal of the atmospheric sciences, applied meteorology and physical oceanography, 134, 1337–1351, 2008.

Beljaars, A. C., Brown, A. R., and Wood, N.: A new parametrization of turbulent orographic form drag, Quarterly Journal of the Royal Meteorological Society, 130, 1327–1347, 2004.

Buizza, R.: The value of probabilistic prediction, Atmospheric Science Letters, 9, 36–42, 2008.

Buizza, R. and Hollingsworth, A.: Storm prediction over Europe using the ECMWF ensemble prediction system, Meteorological Applications, 9, 289–305, 2002.

Buizza, R., Leutbecher, M., and Isaksen, L.: Potential use of an ensemble of analyses in the ECMWF Ensemble Prediction System, Quarterly Journal of the Royal Meteorological Society: A journal of the atmospheric sciences, applied meteorology and physical oceanography, 134, 2051–2066, 2008.

Caracciolo, D., Francipane, A., Viola, F., Noto, L. V., and Deidda, R.: Performances of GPM satellite precipitation over the two major Mediterranean islands, Atmospheric Research, 213, 309–322, 2018.

Carrió, D., Homar, V., Jansa, A., Romero, R., and Picornell, M.: Tropicalization process of the 7 November 2014 Mediterranean cyclone: Numerical sensitivity study, Atmospheric Research, 197, 300–312, 2017.

Carrió, D., Homar, V., Jansà, A., Picornell, M., and Campins, J.: Diagnosis of a high-impact secondary cyclone during HyMeX-SOP1 IOP18, Atmospheric Research, 242, 104 983, 2020.

Cavicchia, L., von Storch, H., and Gualdi, S.: A long-term climatology of medicanes, Climate dynamics, 43, 1183–1195, 2014.

Chaboureau, J. P., Pantillon, F., Lambert, D., Richard, E., and Claud, C.: Tropical transition of a Mediterranean storm by jet crossing, Quarterly Journal of the Royal Meteorological Society, 138, 596–611, https://doi.org/10.1002/qj.960, 2012.

Christensen, H. M., Moroz, I., and Palmer, T.: Stochastic and perturbed parameter representations of model uncertainty in convection parameterization, Journal of the Atmospheric Sciences, 72, 2525–2544, 2015.

Cioni, G., Malguzzi, P., and Buzzi, A.: Thermal structure and dynamical precursor of a Mediterranean tropical-like cyclone, Quarterly Journal of the Royal Meteorological Society, 142, 1757–1766, 2016.

Cioni, G., Cerrai, D., and Klocke, D.: Investigating the predictability of a Mediterranean tropical-like cyclone using a storm-resolving model, Quarterly Journal of the Royal Meteorological Society, 144, 1598–1610, 2018.

Claud, C., Alhammoud, B., Funatsu, B. M., and Chaboureau, J.-P.: Mediterranean hurricanes: large-scale environment and convective and precipitating areas from satellite microwave observations, Natural Hazards and Earth System Sciences, 10, 2199–2213, 2010.

Comellas Prat, A., Federico, S., Torcasio, R. C., D'Adderio, L. P., Dietrich, S., and Panegrossi, G.: Evaluation of the Sensitivity of Medicane Ianos to Model Microphysics and Initial Conditions Using Satellite Measurements, Remote Sensing, 13, 4984, 2021.

Dafis, S., Claud, C., Kotroni, V., Lagouvardos, K., and Rysman, J.-F.: Insights into the convective evolution of Mediterranean tropical-like cyclones, Quarterly Journal of the Royal Meteorological Society, 146, 4147–4169, 2020.

Davis, C.: Resolving tropical cyclone intensity in models, Geophysical Research Letters, 45, 2082–2087, 2018.

Davolio, S., Miglietta, M., Moscatello, A., Pacifico, F., Buzzi, A., and Rotunno, R.: Numerical forecast and analysis of a tropical-like cyclone in the Ionian Sea, Natural Hazards and Earth System Sciences, 9, 551–562, 2009.

Di Muzio, E., Riemer, M., Fink, A. H., and Maier-Gerber, M.: Assessing the predictability of Medicanes in ECMWF ensemble forecasts using an object-based approach, Quarterly Journal of the Royal Meteorological Society, 145, 1202–1217, 2019.

Donlon, C. J., Martin, M., Stark, J., Roberts-Jones, J., Fiedler, E., and Wimmer, W.: The operational sea surface temperature and sea ice analysis (OSTIA) system, Remote Sensing of Environment, 116, 140–158, 2012.

Emanuel, K.: Genesis and maintenance of" Mediterranean hurricanes", Advances in Geosciences, 2, 217–220, 2005.

Emanuel, K. A.: An air-sea interaction theory for tropical cyclones. Part I: Steady-state maintenance, Journal of Atmospheric Sciences, 43, 585–605, 1986.

Ernst, J. and Matson, M.: A Mediterranean tropical storm?, Weather, 38, 332–337, 1983.

Fink, A. H., Pohle, S., Pinto, J. G., and Knippertz, P.: Diagnosing the influence of diabatic processes on the explosive deepening of extratropical cyclones, Geophysical Research Letters, 39, 2012.

Fischer, M. S., Tang, B. H., and Corbosiero, K. L.: Assessing the influence of upper-tropospheric troughs on tropical cyclone intensification rates after genesis, Monthly Weather Review, 145, 1295–1313, 2017.

Fita, L. and Flaounas, E.: Medicanes as subtropical cyclones: The December 2005 case from the perspective of surface pressure tendency diagnostics and atmospheric water budget, Quarterly Journal of the Royal Meteorological Society, 144, 1028–1044, 2018.

Flaounas, E., Raveh-Rubin, S., Wernli, H., Drobinski, P., and Bastin, S.: The dynamical structure of intense Mediterranean cyclones, Climate Dynamics, 44, 2411–2427, 2015.

Flaounas, E., Kotroni, V., Lagouvardos, K., Gray, S. L., Rysman, J.-F., and Claud, C.: Heavy rainfall in Mediterranean cyclones. Part I: contribution of deep convection and warm conveyor belt, Climate dynamics, 50, 2935–2949, 2018.

Flaounas, E., Gray, S. L., and Teubler, F.: A process-based anatomy of Mediterranean cyclones: from baroclinic lows to tropical-like systems, Weather and Climate Dynamics, 2, 255–279, 2021.

Flaounas, E., Davolio, S., Raveh-Rubin, S., Pantillon, F., Miglietta, M. M., Gaertner, M. A., Hatzaki, M., Homar, V., Khodayar, S., Korres, G., et al.: Mediterranean cyclones: Current knowledge and open questions on dynamics, prediction, climatology and impacts, Weather and Climate Dynamics, 3, 173–208, 2022.

Forbes, R. M., Tompkins, A. M., and Untch, A.: A new prognostic bulk microphysics scheme for the IFS, 2011.

Frogner, I.-L., Andrae, U., Ollinaho, P., Hally, A., Hämäläinen, K., Kauhanen, J., Ivarsson, K.-I., and Yazgi, D.: Model uncertainty representation in a convection-permitting ensemble—SPP and SPPT in HarmonEPS, Monthly Weather Review, 150, 775–795, 2022.

Gascón, E., Sandu, I., Vannière, B., Magnusson, L., Forbes, R., Polichtchouk, I., Van Niekerk, A., Sützl, B., Maier-Gerber, M., Diamantakis, M., et al.: Advances towards a better prediction of weather extremes in the Destination Earth initiative, Tech. rep., Copernicus Meetings, 2023.

Geetha, B. and Balachandran, S.: Diabatic heating and convective asymmetries during rapid intensity changes of tropical cyclones over North Indian Ocean, Tropical Cyclone Research and Review, 5, 32–46, 2016.

Grabowski, W. W., Wu, X., and Moncrieff, M. W.: Cloud resolving modeling of tropical cloud systems during Phase III of GATE. Part III: Effects of cloud microphysics, Journal of the atmospheric sciences, 56, 2384–2402, 1999.

Hamill, T. M., Whitaker, J. S., Fiorino, M., and Benjamin, S. G.: Global ensemble predictions of 2009's tropical cyclones initialized with an ensemble Kalman filter, Monthly Weather Review, 139, 668–688, 2011.

Hart, R. E.: A cyclone phase space derived from thermal wind and thermal asymmetry, Monthly weather review, 131, 585–616, 2003.

870 Hart, R. E. and Evans, J. L.: A climatology of the extratropical transition of Atlantic tropical cyclones, Journal of Climate, 14, 546–564, 2001.

Hogan, R. J. and Bozzo, A.: A flexible and efficient radiation scheme for the ECMWF model, Journal of Advances in Modeling Earth Systems, 10, 1990–2008, 2018.

Homar, V., Romero, R., Stensrud, D., Ramis, C., and Alonso, S.: Numerical diagnosis of a small, quasi-tropical cyclone over the western
875 Mediterranean: Dynamical vs. boundary factors, Quarterly Journal of the Royal Meteorological Society: A journal of the atmospheric sciences, applied meteorology and physical oceanography, 129, 1469–1490, 2003.

Huffman, G. J., Bolvin, D. T., Braithwaite, D., Hsu, K.-L., Joyce, R. J., Kidd, C., Nelkin, E. J., Sorooshian, S., Stocker, E. F., Tan, J., et al.: Integrated multi-satellite retrievals for the global precipitation measurement (GPM) mission (IMERG), in: Satellite precipitation measurement, pp. 343–353, Springer, 2020.

880 IFS Documentation CY47R3, E.: IFS Documentation CY47R3 Part IV Physical processes, 2021a.

IFS Documentation CY47R3, E.: IFS Documentation CY47R3 Part V Ensemble prediction system, 2021b.

IFS Documentation CY47R3, E.: IFS Documentation CY47R3 Part VII ECMWF Wave model, 2021c.

Köhler, M., Ahlgrimm, M., and Beljaars, A.: Unified treatment of dry convective and stratocumulus-topped boundary layers in the ECMWF model, Quarterly Journal of the Royal Meteorological Society, 137, 43–57, 2011.

885 Koseki, S., Mooney, P. A., Cabos, W., Gaertner, M. Á., de la Vara, A., and González-Alemán, J. J.: Modelling a tropical-like cyclone in the Mediterranean Sea under present and warmer climate, Natural Hazards and Earth System Sciences, 21, 53–71, 2021.

Lagouvardos, K., Karagiannidis, A., Dafis, S., Kalimeris, A., and Kotroni, V.: Ianos—A hurricane in the Mediterranean, Bulletin of the American Meteorological Society, 103, E1621–E1636, 2022.

Lang, S., Leutbecher, M., and Jones, S.: Impact of perturbation methods in the ECMWF ensemble prediction system on tropical cyclone
890 forecasts, Quarterly Journal of the Royal Meteorological Society, 138, 2030–2046, 2012.

Lang, S. T., Lock, S.-J., Leutbecher, M., Bechtold, P., and Forbes, R. M.: Revision of the stochastically perturbed parametrisations model uncertainty scheme in the integrated forecasting system, Quarterly Journal of the Royal Meteorological Society, 147, 1364–1381, 2021.

Leutbecher, M., Lock, S.-J., Ollinaho, P., Lang, S. T., Balsamo, G., Bechtold, P., Bonavita, M., Christensen, H. M., Diamantakis, M., Dutra, E., et al.: Stochastic representations of model uncertainties at ECMWF: State of the art and future vision, Quarterly Journal of the Royal
895 Meteorological Society, 143, 2315–2339, 2017.

Lin, J. and Qian, T.: Rapid intensification of tropical cyclones observed by AMSU satellites, Geophysical Research Letters, 46, 7054–7062, 2019.

Magnusson, L., Thorpe, A., Buizza, R., Rabier, F., and Nicolau, J.: Predicting this year's European heat wave, ECMWF Newsletter, 145, 4–5, 2015.

900 Majumdar, S. J. and Torn, R. D.: Probabilistic verification of global and mesoscale ensemble forecasts of tropical cyclogenesis, Weather and Forecasting, 29, 1181–1198, 2014.

Majumdar, S. J., Magnusson, L., Bechtold, P., Bidlot, J.-R., and Doyle, J. D.: Advanced tropical cyclone prediction using the experimental global ECMWF and operational regional COAMPS-TC systems, Monthly weather review, 2023.

Malardel, S., Wedi, N., Deconinck, W., Diamantakis, M., Kühnlein, C., Mozdzynski, G., Hamrud, M., and Smolarkiewicz, P.: A new grid for
905 the IFS, ECMWF newsletter, 146, 321, 2016.

Mazza, E., Ulbrich, U., and Klein, R.: The tropical transition of the October 1996 medicane in the western Mediterranean Sea: A warm seclusion event, Monthly Weather Review, 145, 2575–2595, 2017.

Miglietta, M., Laviola, S., Malvaldi, A., Conte, D., Levizzani, V., and Price, C.: Analysis of tropical-like cyclones over the Mediterranean Sea through a combined modeling and satellite approach, Geophysical Research Letters, 40, 2400–2405, 2013.

910 Miglietta, M., Cerrai, D., Laviola, S., Cattani, E., and Levizzani, V.: Potential vorticity patterns in Mediterranean "hurricanes", Geophysical Research Letters, 44, 2537–2545, 2017.

Miglietta, M. M. and Rotunno, R.: Development mechanisms for Mediterranean tropical-like cyclones (medicanes), Quarterly Journal of the Royal Meteorological Society, 145, 1444–1460, 2019.

Miglietta, M. M., Moscatello, A., Conte, D., Mannarini, G., Lacorata, G., and Rotunno, R.: Numerical analysis of a Mediterranean 'hurri-

915 cane'over south-eastern Italy: Sensitivity experiments to sea surface temperature, Atmospheric research, 101, 412–426, 2011.

Miglietta, M. M., Mastrangelo, D., and Conte, D.: Influence of physics parameterization schemes on the simulation of a tropical-like cyclone in the Mediterranean Sea, Atmospheric Research, 153, 360–375, 2015.

Mogensen, K., Keeley, S., and Towers, P.: Coupling of the NEMO and IFS models in a single executable, ECMWF Reading, United Kingdom, 2012.

920 Montani, A., Cesari, D., Marsigli, C., and Paccagnella, T.: Seven years of activity in the field of mesoscale ensemble forecasting by the COSMO-LEPS system: main achievements and open challenges, Tellus A: Dynamic Meteorology and Oceanography, 63, 605–624, 2011.

Moscatello, A., Marcello Miglietta, M., and Rotunno, R.: Observational analysis of a Mediterranean'hurricane'over south-eastern Italy, Weather, 63, 306, 2008.

Munsell, E. B., Zhang, F., and Stern, D. P.: Predictability and dynamics of a nonintensifying tropical storm: Erika (2009), Journal of the

925 atmospheric sciences, 70, 2505–2524, 2013.

Noyelle, R., Ulbrich, U., Becker, N., and Meredith, E. P.: Assessing the impact of sea surface temperatures on a simulated medicane using ensemble simulations, Natural Hazards and Earth System Sciences, 19, 941–955, 2019.

Ollinaho, P., Lock, S.-J., Leutbecher, M., Bechtold, P., Beljaars, A., Bozzo, A., Forbes, R. M., Haiden, T., Hogan, R. J., and Sandu, I.: Towards process-level representation of model uncertainties: stochastically perturbed parametrizations in the ECMWF ensemble, Quarterly Journal

930 of the Royal Meteorological Society, 143, 408–422, 2017.

Palmen, E.: On the formation and structure of tropical hurricanes, Geophysica, 3, 26–38, 1948.

Palmer, T. N., Buizza, R., Doblas-Reyes, F., Jung, T., Leutbecher, M., Shutts, G. J., Steinheimer, M., and Weisheimer, A.: Stochastic parametrization and model uncertainty, 2009.

Panegrossi, G., D'Adderio, L. P., Dafis, S., Rysman, J.-F., Casella, D., Dietrich, S., and Sanò, P.: Warm Core and Deep Convection in

935 Medicanes: A Passive Microwave-Based Investigation, Remote Sensing, 15, 2838, 2023.

Pantillon, F., Chaboureau, J.-P., Mascart, P., and Lac, C.: Predictability of a Mediterranean tropical-like storm downstream of the extratropical transition of Hurricane Helene (2006), Monthly Weather Review, 141, 1943–1962, 2013.

Peinó, E., Bech, J., and Udina, M.: Performance Assessment of GPM IMERG Products at Different Time Resolutions, Climatic Areas and Topographic Conditions in Catalonia, Remote Sensing, 14, 5085, 2022.

940 Picornell, M., Campins, J., and Jansà, A.: Detection and thermal description of medicanes from numerical simulation, Natural Hazards and Earth System Sciences, 14, 1059–1070, 2014.

Portmann, R., González-Alemán, J. J., Sprenger, M., and Wernli, H.: How an uncertain short-wave perturbation on the North Atlantic wave guide affects the forecast of an intense Mediterranean cyclone (Medicane Zorbas), Weather and Climate Dynamics, 1, 597–615, 2020.

Pytharoulis, I.: Analysis of a Mediterranean tropical-like cyclone and its sensitivity to the sea surface temperatures, Atmospheric Research,

945 208, 167–179, 2018.

Pytharoulis, I., Craig, G. C., and Ballard, S. P.: The hurricane-like Mediterranean cyclone of January 1995, Meteorological Applications: A journal of forecasting, practical applications, training techniques and modelling, 7, 261–279, 2000.

Rabier, F., Järvinen, H., Klinker, E., Mahfouf, J.-F., and Simmons, A.: The ECMWF operational implementation of four-dimensional variational assimilation. I: Experimental results with simplified physics, Quarterly Journal of the Royal Meteorological Society, 126, 1143–1170, 2000.

Ragone, F., Mariotti, M., Parodi, A., Von Hardenberg, J., and Pasquero, C.: A climatological study of western mediterranean medicanes in numerical simulations with explicit and parameterized convection, Atmosphere, 9, 397, 2018.

Rasmussen, E. and Zick, C.: A subsynoptic vortex over the Mediterranean with some resemblance to polar lows, Tellus A, 39, 408–425, 1987.

Raveh-Rubin, S. and Flaounas, E.: A dynamical link between deep Atlantic extratropical cyclones and intense Mediterranean cyclones, Atmospheric Science Letters, 18, 215–221, 2017.

Ricchi, A., Miglietta, M. M., Bonaldo, D., Cioni, G., Rizza, U., and Carniel, S.: Multi-physics ensemble versus atmosphere–ocean coupled model simulations for a tropical-like cyclone in the Mediterranean Sea, Atmosphere, 10, 202, 2019.

Romero, R. and Emanuel, K.: Medicane risk in a changing climate, Journal of Geophysical Research: Atmospheres, 118, 5992–6001, 2013.

Tiedtke, M.: A comprehensive mass flux scheme for cumulus parameterization in large-scale models, Monthly weather review, 117, 1779–1800, 1989.

Tiedtke, M.: Representation of clouds in large-scale models, Monthly Weather Review, 121, 3040–3061, 1993.

Torn, R. D. and Cook, D.: The role of vortex and environment errors in genesis forecasts of Hurricanes Danielle and Karl (2010), Monthly weather review, 141, 232–251, 2013.

Vich, M., Romero, R., and Brooks, H.: Ensemble prediction of Mediterranean high-impact events using potential vorticity perturbations. Part I: Comparison against the multiphysics approach, Atmospheric research, 102, 227–241, 2011.

Wimmer, M., Rivière, G., Arbogast, P., Piriou, J.-M., Delanoë, J., Labadie, C., Cazenave, Q., and Pelon, J.: Diabatic processes modulating the vertical structure of the jet stream above the cold front of an extratropical cyclone: sensitivity to deep convection schemes, Weather and Climate Dynamics, 3, 863–882, 2022.

Yanai, M., Esbensen, S., and Chu, J.-H.: Determination of bulk properties of tropical cloud clusters from large-scale heat and moisture budgets, Journal of Atmospheric Sciences, 30, 611–627, 1973.

Zhang, W., Villarini, G., Vecchi, G. A., and Murakami, H.: Rainfall from tropical cyclones: high-resolution simulations and seasonal forecasts, Climate dynamics, 52, 5269–5289, 2019.

Zhang, W., Villarini, G., Scoccimarro, E., and Napolitano, F.: Examining the precipitation associated with medicanes in the high-resolution ERA-5 reanalysis data, International Journal of Climatology, 41, E126–E132, 2021.

Zimbo, F., Ingemi, D., and Guidi, G.: The tropical-like cyclone "ianos" in September 2020, Meteorology, 1, 29–44, 2022.